Transportation Geotechnics 49 (2024) 101388

Contents lists available at ScienceDirect

Transportation Geotechnics

journal homepage: www.elsevier.com/locate/trgeo

A review of soil deformation and lateral pressure ratcheting phenomena in integral abutment bridges

M.S.K. Hassan *, D.S. Liyanapathirana, W. Fuentes, C.J. Leo, P. Hu

School of Engineering, Design and Built Environment, Western Sydney University, 2751, Australia

A R T I C L E I N F O

Keywords:
Integral bridges
Soil-structure interaction
Lateral stress ratcheting
Soil deformation
Mitigative strategies
Review

A B S T R A C T

Integral bridges have been proposed as a jointless design alternative to the traditional counterparts, possessing copious potential economic and structural advantages. However, due to the monolithic connection at the girder-abutment interface, longitudinal deformations from the superstructure must now be accommodated by the stiffness of the approach backfill and soil surrounding the foundation. Consequently, in addition to traffic loads, integral bridge approaches are subjected to long-term, cyclic loading due to diurnal and seasonal thermal variations. This has resulted in two progressive geotechnical phenomena: an escalation of lateral passive pressures at the abutment-soil interface and accumulated deformations near the bridge approach. Over the last two decades, several investigations on the approach backfill-abutment interaction have been carried out. However, previous reviews on integral bridges have not comprehensively discussed the theoretical aspects of these two complex geotechnical issues. Hence, this paper presents a discussion on the long-term response of stress ratcheting observed from controlled analyses, along with a comparison to that from field monitoring data. Subsequently, the occurrence of accumulated deformations, along with a correlation to the mechanism of the cyclic interaction is explored. The effects of foundation design choice and skew angle on the passive pressure accumulation and soil deformation behavior are then presented. Subsequently, approaches used to mitigate the effects of the backfill-abutment interaction are compared. From this review, it is apparent that outcomes based on available experimental and field investigations are yet inadequate to develop analytical models required to predict the long-term response of integral bridge approach backfills under various loading conditions.

Introduction

With the increasing rate of vehicle production and corresponding growth in highway infrastructure [98], the requirement and development of economic, robust, and durable bridge structures are crucial. As illustrated in Fig. 1 (a), traditional bridges of this era utilize movement joints at the abutment-girder and deck-approach slab interfaces. However, due to the ingress of de-icing salts and chemicals, accumulation of debris, water leaks, along with the ever-increasing traffic loading, these expansion joints are subjected to significant durability complications [90,137]. As a result, jointed bridges require frequent time-intensive maintenance works [21,40], which if not addressed can lead to progressive corrosion issues and additional structural stresses [126]. Surveys have demonstrated that joint maintenance is an exorbitant source of operational expense [52], resulting in an additional annual expenditure of approximately $100 million [69]. Further, the requirement of recurring maintenance also signifies inherent disruptions to traffic flow, especially in freeways and arterial roads [15]. The above reasons coupled with the development of structural analysis software have motivated the design and use of jointless bridges [52].

In essence, integral bridges are those in which the superstructure and substructure are monolithically connected, effectively eliminating the use of expansion joints. A schematic of an integral bridge has been shown in Fig. 1 (b). It should be noted that integral bridges can be subcategorized to three primary variants: integral abutment bridges (IABs, also used interchangeably with full-integral abutment bridges (FIABs)), semi-integral abutment bridges (SIABs) and deck-extension bridges [138,64,6]. In this study, attention will be given specifically to the behavior of full-integral and semi-integral bridges, which do not possess girder-abutment expansion joints (refer to annotation ii in Fig. 1 (b)). The absence of expansion joints in integral bridges have yielded various economic and performance benefits: (1) relatively low capital expense due to simpler continuous design [92,96]; (2) comparatively swifter construction time, along with significant operational cost

* Corresponding author.
E-mail address: m.kaizerhassan@westernsydney.edu.au (M.S.K. Hassan).

https://doi.org/10.1016/j.trgeo.2024.101388
Received 30 January 2024; Received in revised form 2 August 2024; Accepted 23 September 2024
Available online 26 September 2024

savings, making it a sustainable option for bridge replacement and retrofitting [63]; (3) requirement of lesser number of piles when compared to equivalent jointed counterparts [63]; (4) enhanced seismic stability, particularly against longitudinal seismic forces [82,1]; and (5) improved distribution of lateral loads, increasing the structural redundancy of the bridge [75]. Collectively, these advantages have led to an increase in global acceptance and usage of the integral bridge design concept [34,85,131].

Due to the presence of a continuous connection, however, any form of longitudinal deck action (due to secondary loads from post-construction shortening, prestressing, seismic, thermal effects, etc.) is now transferred to the substructure, i.e., the abutments and foundation, prompting a soil-structure interaction (SSI) [61]. As a result, due to the fluctuation of ambient temperatures with the progression of seasonal cycles, integral bridge abutments are subject to complex cyclic movements that occur throughout the lifespan of the structure [9]. Amongst several other performance complications, this has led to two detrimental geotechnical consequences. The first is the accumulation of passive pressures on the abutment wall, a phenomenon known as lateral stress-ratcheting [141,44]. This concurrently results in a simultaneous rise of internal forces within the other structural members of the bridge [80]. The other issue of paramount importance is the soil deformation that occurs in the approach backfill, wherein a gradual development of soil subsidence can be observed [78]. These occurrences have resulted in the imposition of strict geometric restrictions such as the allowable bridge length, skew angle, and abutment height [106]. Collectively, these drawbacks have ultimately undermined the true potential of this concept and as such, integral bridges have become a topic of interest in the geotechnical and structural research communities.

While considerable research effort has been made utilizing numerical techniques (e.g., Stastny et al. [114], Sakhare et al. [102], Silva et al. [109], Fu et al. [36], Verma and Mishra [122], Razmi and McCabe [101], Sandberg et al. [103]), experimental models (e.g., Makino et al. [81], Luo et al. [78], Sigdel et al. [107], Liu et al. [73]) and field instrumentation (e.g., Alhowaidi et al. [10], Laaksonen [60], Mofarraj and Zornberg [87]), limited attention has been given towards communicating the fundamental causes behind the temperature-induced SSI effects. Further, it is evident that the impact of certain determining design parameters such as bridge skew and foundation design option require supplemental evaluation. Moreover, while review papers on the overall concept of integral bridges have been conducted, these investigations have focused on other aspects. For example, recent reviews carried out by Vasconez et al. [121], Sigdel et al. [105] and Tabatabai et al. [116], have principally concentrated on the current design guidelines, highlighting the lack of coherence in international legislative practice. Mitoulis [85] and Dhar and Dasgupta [28] presented detailed reviews on the seismic SSI of integral bridges. As such, this study aims to provide the current state of knowledge on specific issues pertaining to the thermal-induced backfill-abutment interaction of integral bridges, highlighting the limitations in previously adopted research methodologies and to provide a scope on the future direction of research.

The paper begins with a critical evaluation and comparison of the long-term response of passive pressure ratcheting from literature on experimental analyses and field instrumentation data. Subsequently, the long-term soil deformation behavior of integral bridge approach backfills is addressed and correlated to a potential soil-structure interaction mechanism. Following this, literature on two key factors, bridge skew and abutment movement mode is analyzed. The approaches used to minimize the cyclic backfill-abutment interaction effects are then evaluated. Finally, the manuscript concludes with the major deductions, and presents recommendations for future investigation directions that will enable for a better prediction of the SSI behavior of integral bridges.

Long-term passive lateral stress accumulation

Trends observed through laboratory experiments

Numerous controlled analyses (experimental and numerical) have been conducted in the last 3 decades to examine and potentially quantify the passive lateral pressure response in integral abutment bridges. It

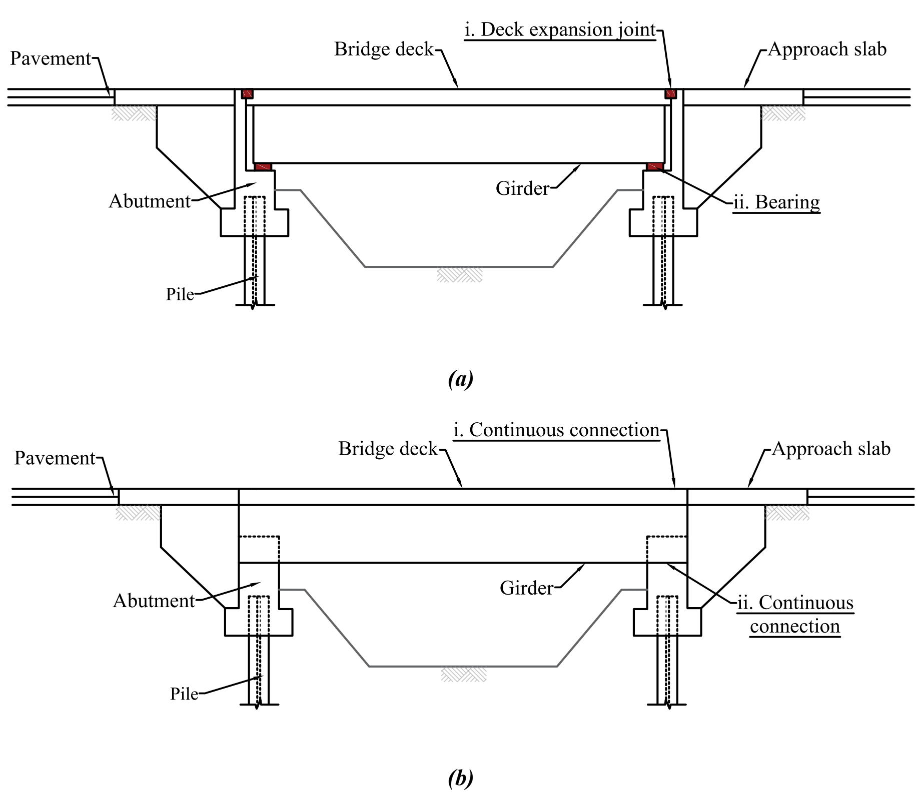

Fig. 1. Schematic example of (a) traditional jointed bridge and (b) integral abutment bridge.

should be noted, however, that unless stated otherwise, the literature reviewed in this study is that of an experimental (or field instrumented) nature. This is due to the inherent limitations of commonly used constitutive relations to predict the mechanical response of granular soils when subject to lateral cyclic straining [37]. While it has been unequivocally accepted that the induced passive stresses have some positive correlation with the number of thermal cycles [77,74,71,46,125], there are certain noteworthy differences in the behavioral trend that should be addressed. Through the use of small-scale physical models, England et al. [32] observed that a majority of the increase in passive pressures occurred within the initial 10 cycles. Following which, the rate of increase in passive pressures reduced significantly and reached a steady state within 120 loading cycles. Similar trends were also observed in scaled physical model tests conducted by Tatsuoka et al. [118] and Sigdel et al. [107] (refer solid line plots in Fig. 2). The initial rapid escalation in lateral pressures is caused by the large active failures and consequential hardening response due to the compressive strains during the passive wall movement [7]. In subsequent active phases, the presence of soil already occupying the voids from the previous active wall movement, along with the increasingly stiffer soil, results in a gradual decrease of soil slumping. England et al. [32] stated that an eventual stabilization of the passive pressure accumulation is due to a presence of a shakedown limit, where the opposing phenomena of soil deformation and dilation are balanced. However, this statement is not technically sound, as a more recent study indicates that in certain cases, dilative behavior continues to progress, even at latter cycles (discussed in Sec. 3). This can be postulated to be because the soil-structure interaction of integral bridges not only involves densification, but also entails fabric development. The term 'fabric development' can be defined as the rearranging and increase in particle contacts that occur as a result of the rolling of granular particles during cyclic shearing [136,134,135,24].

In certain experiments, an asymptote is not apparent within 120 cycles of thermal loading (refer dashed line plots in Fig. 2). Tapper and Lehane [117], through centrifuge tests, observed that for a normalized abutment movement, Δ/H, (Δ is the abutment displacement magnitude as depicted through Fig. 6 and H is the abutment height) of $\pm$ 0.63 %, passive pressures continued to increase for 1000 cycles. Here, the peak pressure increased from 150.7 kPa in cycle 100 to 177.6 kPa in cycle 1000. Comparable behavior has been noted in other studies such as that by Sigdel et al. [108]. This response is likely due to the magnitude of abutment displacement, and is evident from Fig. 3 (a) to (c). Herein, the variation in the increase of the passive pressure coefficient from various experimental investigations at different abutment displacements have been depicted. It should be noted that while an attempt has been made here to normalize the results, further generalization of the time-history of the increase in pressure coefficient across various studies is not possible due to the dependency on other loading conditions such as movement mode (discussed in Sec. 4), soil properties [3,2,129], abutment stiffness [89,89] and model scale [130]. Regardless, the comparison indicates that at greater abutment movement amplitudes, not only is the passive pressure due to a greater monotonic displacement larger, but a more substantial accumulation from cycle-to-cycle can be expected. Further, at larger displacements, the number of cycles required to reach a theoretical limit state is higher. This is potentially because greater movement amplitudes lead to greater active failures, particle rolling and hence allowing greater fabric development. From a practical standpoint, this suggests that longer integral bridges will continue to experience considerable stress ratcheting throughout the lifespan of the structure, thus requiring appropriate mitigative measures (refer Sec. 6). These observations also highlight that experimental/numerical investigations which only consider 10–50 loading cycles, do not provide the critical loading case of passive lateral stresses acting on the abutment wall, particularly for longer IABs.

This non-linear relationship between bridge length and long-term lateral stress accumulation also provides a rationale as to why legislative guidelines such as the PD 6694–1[16] have been remarked in the literature (e.g., Luo et al. [77], Banks and Bloodworth [12]) to be not adequate to describe the critical passive pressures for a wide range of bridge lengths. An example of this issue has been demonstrated through Fig. 4 (a), which differentiates the passive pressure distribution obtained through the centrifuge model results presented in Tapper and Lehane [117] to that recommended by the PD 6694–1 [16] guideline. The peak friction angle ($\varphi_{peak} = 37.7°$) needed for the calculations were obtained from triaxial tests on UWA superfine silica sand performed by Chow et al. [22], and the wall deflection (d_d) was computed as 2 mm ($\Delta/H = 0.05$ %), 8 mm ($\Delta/H = 0.2$ %) and 25.2 mm ($\Delta/H = 0.63$ %). While the guideline is able to predict the lateral pressure profile reasonably well, the magnitudes display considerable disparity to the experimental data. At increasing abutment movement amplitudes, the PD 6694–1 is increasingly unconservative, highlighting its incapability to capture the behavior of integral bridge approach backfills. This concern also applies to other guidelines such as the NZ Transport Agency research report 577 [131] used in New Zealand, as well as the BTN 010 [123] and the Design Criteria for Bridges and Other Structures Manual [99] used in various states of Australia, as these refer back to the propositions made in the PD 6694–1 [16]. In Canada and the USA, there is a lack of standardized guidelines, with each state Department of Transportation (DOT) possessing a respective design manual to guide local engineers [121,116]. From a review of the DOT manuals, it is evident that in a majority of cases, there is no explicit guidance for the determination of lateral pressure, leading to either the use of empiricism or classical earth pressure

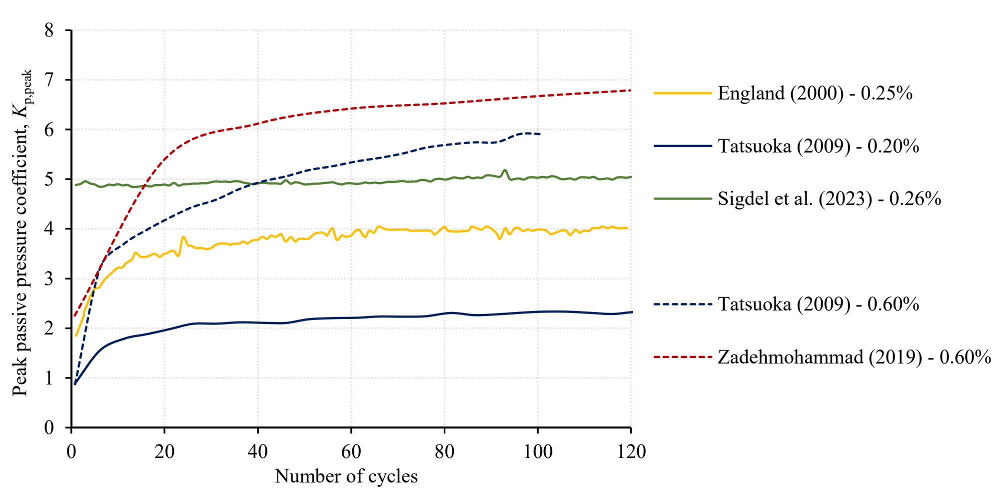

Fig. 2. Peak passive pressure accumulation with progression of loading cycles.

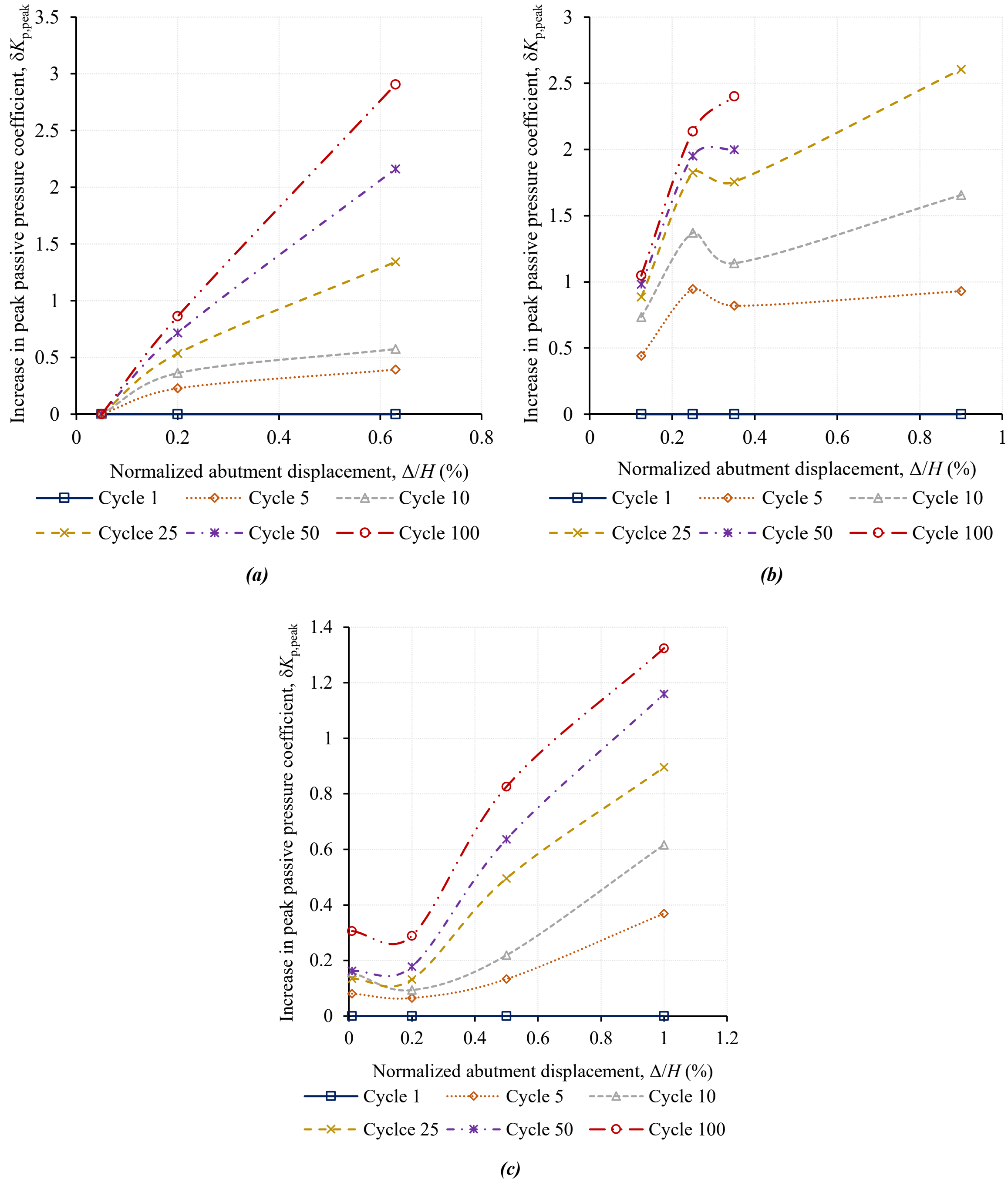

Fig. 3. Variation of increase in peak passive lateral pressure coefficient with abutment movement magnitude from (a) Lehane [66] where $H = 4$ m, (b) England et al. [32] where $H = 0.57$ m, and (c) Springman et al. [113] where $H = 6$ *m*.

theories based on monotonic loading conditions [105]. An example of this has been illustrated in Fig. 4 (a), which also includes a comparison with lateral pressures predicted by the Massachusetts Department of Transportation LRFD Bridge Manual [83]. Here, the MassDOT guideline assumes a linear variation in the lateral stress profile, and considerable overestimations of stresses, particularly along the lower half of the abutment are apparent. This will lead to discrepancies in the corresponding bending moment distribution, which will in turn impact the structural design of the integral abutment. The limitations of current design guidelines are further highlighted through Fig. 4 (b). Herein, passive pressure coefficients at the peak pressure positions (K_{exp}) from numerous experimental [7,9,32,66,77,78,88,106,108,118,140] studies are compared to the following theoretical pressure coefficients (K_{theory}): MassDOT [83], PD 6694–1 [16], Rankine's pressure theory [100] and Coulomb's pressure theory [26]. It should be noted that for cases in which φ_{peak} could not be determined, the critical state friction angle was used to compute K_d^* from PD 6694–1. It is apparent that all theoretical pressure coefficients exhibit considerable variance at a range of abutment displacement magnitudes. Hence, collectively, there is a clear requirement to amend existing guidelines and develop a new simple means to predict the passive lateral pressures that would occur due to thermal-induced deck deformations in IABs.

Lateral stress escalation in field integral bridges

Controlled analysis techniques offer a comparatively simpler means

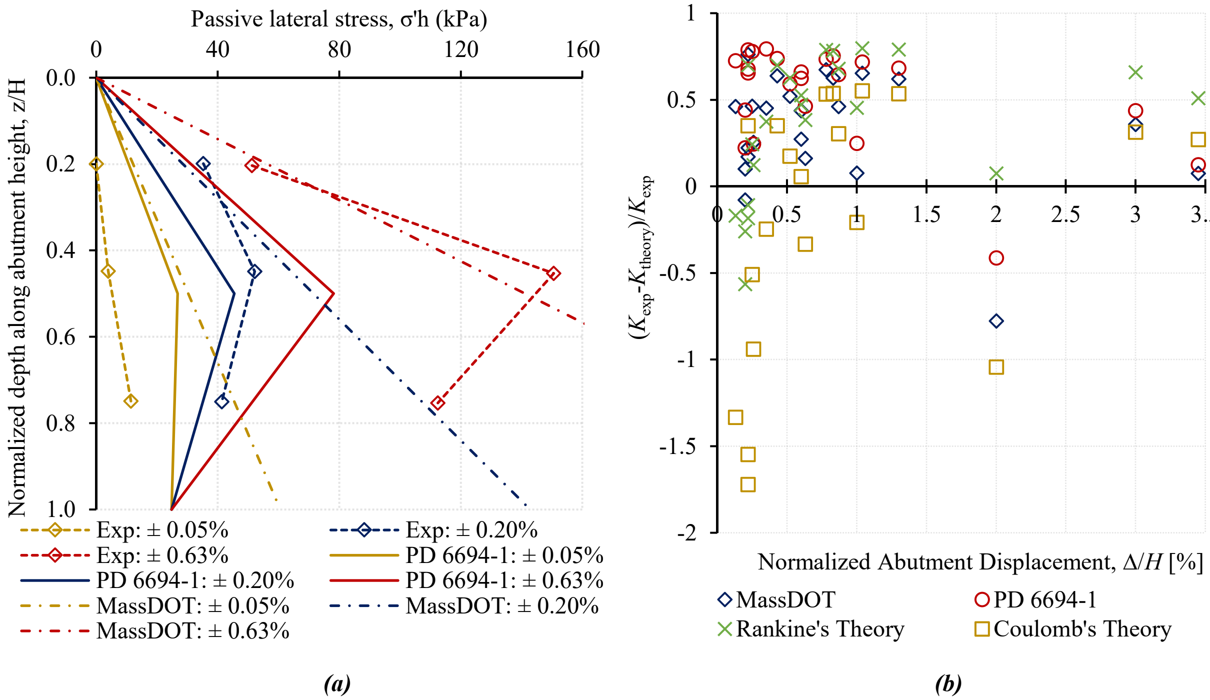

Fig. 4. Comparison between (a) lateral pressure profiles from Tapper and Lehane [117] to that predicted using the PD 6694–1 and MassDOT LRFD Bridge Manual, and (b) peak passive earth pressure coefficients from various experimental studies to that predicted by four selected theoretical passive pressure coefficients.

to assess the soil-structure interaction of integral bridges. However, the corresponding assumptions should be considered when evaluating the obtained results. Such assumptions include the mechanical response of soils in scaled models and the loading/deformation rate of the bridge (one year for one cycle in the field in comparison to hours/minutes in the model). Hence, a discussion and juxtaposition of integral bridge behavior under both conditions is vital towards developing a complete understanding of these structures. Due to this requirement to examine the behavior of integral bridges pertaining to practical conditions, field instrumentation and monitoring have been carried out extensively. Recent reviews by Chen et al. [20] and Liu et al. [75] indicate that to knowledge, there are more than 45 cases of integral bridges across the globe, which are being used to perform (or have conducted) monitoring efforts. However, unlike from controlled analyses, the stress ratcheting phenomenon is not always evident, leading some literature to question the requirement for consideration of lateral pressure build-up during bridge design. When considering shorter IABs (length < 50 m), from an analysis of a 41.3 m (135 ft) semi-integral abutment bridge in South Korea, Kim et al. [56] reported no stress escalation over a 34-month period. Civjan et al. [23] presented field data for two composite integral abutment bridges in the USA, spanning 43 m (141 ft) and 37 m (121 ft) in length. Here, over the course of a 2.5-year monitoring period, soil softening behavior is observed. Similar responses were noted by Ooi et al. [94] where data for a 24.4 m (80 ft) long concrete integral bridge in Hawaii is presented. These seemingly unexpected responses could be due to a combination of numerous causes; stress ratcheting is inherently not significant for shorter bridges due to smaller cyclic deformation magnitudes, presence of site-specific conditions such as frost build-up (e.g., Kim et al. [56] noted temperature minimums of around −7 °C) and hydrostatic loading, and creep and shrinkage effects result in a net negative volumetric strain, inhibiting stress ratcheting. In some longer IABs, however, an annual accumulation of lateral stresses is present. An instance of this is discernible from the data presented on the Scotch-Road Bridge, which is a 91.4 m (300 ft) long steel integral abutment bridge [55,54,38]. Herein, the peak passive pressure coefficient almost doubled (from 2.06 to 4.20) over a period of 3 years, followed by a gradual increase to 4.31 in the final year of monitoring. Comparable observations were made by Huntley and Valsangkar [47] and Huntley and Valsangkar [48], where for a 76 m concrete integral bridge, a gradual rise in passive pressures over 9 years was observed for one of the abutments. Similar findings have been noted from other IABs as stated in the works of Bonczar et al. [13], Hoppe [42], Frosch and Lovell [35], Kim and Laman [57], Pétursson and Kerokoski [97], Skorpen et al. [111], Mofarraj and Zornberg [86], etc. Collectively, stress accumulation seems to be present and more prevalent in longer bridges, which is unsurprising given the relationships discussed in Sec. 2.1. However, to the authors' knowledge, the maximum duration of available field instrumentation data for an integral bridge is 9 years, which given the design life of bridges and the progressive nature of the stress ratcheting phenomenon, is insufficient to derive conclusions on the severity of long-term stress build-up at field conditions.

A notable variation between field IABs and controlled tests, however, is that the models generally estimate a much higher degree of passive pressure accumulation relative to that observed in the field. While there could be numerous potential reasons for this, a determining variable is the magnitude of abutment displacement. In most experimental research involving the behavior of integral bridges, comparisons are made assuming that the abutment movement corresponds to that predicted by the equation of linear unrestrained thermal expansion as indicated below:

$$\Delta l = l_0 \alpha \Delta T \quad (1)$$

where Δl is the change in length, l_0 is the original length, α is the linear coefficient of thermal expansion and ΔT is the variation in temperature.

However, in reality, the longitudinal movements of the bridge superstructure are restricted by the foundation and surrounding soil, abutment and backfill [58,11]. Through field instrumentation, Wendner and Strauss [127] determined that actual abutment movement was only 42% of that predicted by free thermal expansion. Similar conclusions have been made by LaFave et al. [61], LaFave et al. [62] and Breña et al. [14]. Further, use of Eqn. (1) also assumes that air temperature is equivalent to the internal temperature of the bridge deck and girders.

However, the effective bridge temperature is in fact impacted by the complex superstructure geometry, use of various construction materials (due to different thermal expansion coefficients), solar radiation [20], underground water [4], thermal inertia [57], etc. An example of the impact of superstructure cross-section on the effective bridge temperature has been demonstrated through the field instrumentation data presented in Skorpen et al. [112]. Here, a 90.45 m reinforced concrete IAB was designed considering linear free thermal expansion, which with a design temperature variation of 3 °C to 45 °C resulted in a longitudinal deformation of 51 mm. However, due to thermal damping effects of the solid girders, a considerable temperature gradient was observed, with temperatures near the bottom of the beam exhibiting relatively minimal variations [110]. This resulted in effective bridge temperature fluctuations of just 3.2 °C to 35.3 °C, which is notably smaller than the design limits [112]. Examples of longitudinal deformation formulae considering some of these factors have been proposed by Oesterle and Volz [93], Abid et al. [5] and Lin et al. [67], and are specific to the geographical location. Hence, while it may be challenging to conduct a reliable long-term field instrumentation of an integral bridge, better predictions of the stress ratcheting phenomenon can be obtained through modelling by taking the above into consideration.

Long-term soil deformation response and soil-structure interaction mechanism

Soil deformation is another geotechnical consequence that occurs as a result of the cyclic backfill-abutment interaction. A discussion of literature on this issue is vital as it not only allows for the development of potential mitigative strategies, but also provides supplementary information on the mechanism of the lateral stress ratcheting occurrence. From a review of available literature, however, it is evident that relative to the investigations on lateral pressure, fewer studies have been conducted on soil deformation in integral bridges. Further, it should be noted that this section only evaluates research from controlled analyses, because field monitoring data on IAB backfill deformations is very limited.

As illustrated through Fig. 5 (a), soil deformation occurring in integral bridges typically consists of two components: soil subsidence directly adjacent to the abutment wall, along with soil upheaval at some distance away from the wall. Considering the former, investigations by Alqarawi et al. [7], Sigdel et al. [108] and England et al. [32] have observed the following mutual key points; the settlement trough (combination of settlement magnitude and zone of settlement) develops in the region between the abutment wall and active failure surface (blue line in Fig. 5 (a)); maximum settlement progresses non-linearly with each cycle at a gradually decreasing rate; and settlement magnitude is greatest when the abutment is at the active position of each cycle. Using particle image velocimetry (PIV) techniques, it has been determined that the cumulative response is due to the non-equivalent deformations experienced by the backfill during the active and passive phases of the abutment movement [77,25]. As the bridge contracts, the soil deforms in an inclined vertical direction as part of a small active wedge and in the subsequent bridge expansion, the compressive strain is primarily in the horizontal direction [118]. Similar to lateral pressure escalations in integral bridges, the magnitude of soil settlement has a positive correlation with the magnitude of abutment displacement (or bridge length and/or temperature differential) [70,117,25,113]. This is because larger abutment amplitudes result in more severe active failures and greater compressive strains. A notable contradiction, however, is the existence of a limiting state for maximum settlement. Numerous studies have stated that while the rate of increase in settlement decreases with each cycle, there seems to be no indication of an approaching limit state [78,39]. However, in a more recent investigation carried out by Sigdel et al. [108], maximum settlement was observed to stabilize during the latter cycles. Potential causes for this variation include the scaling of the experiments and abutment movement mode (discussed in Sec. 4.1). For example, the testing rig employed by England et al. [32] retained a backfill with a height equivalent to approximately a third of that in Sigdel et al. [108], which given the barotropic nature of soils, can result in a different mechanical response. Moreover, the studies conducted by Luo et al. [78] and Al-Qarawi et al. [9] involve a relatively lesser number of cycles (12 and 30 cycles, respectively), whereas Sigdel et al. [108] only observed a limit state after 75 cycles.

In some instances, the backfill exhibits dilative behavior in the form of soil heaving and is typically observed to occur in the region delineated by the active and passive failure (green line in Fig. 5 (a)) surfaces. Through numerical investigations, Al-Qarawi et al. (2016) and England et al. [32] noted that this could be due to the greater dilatancy

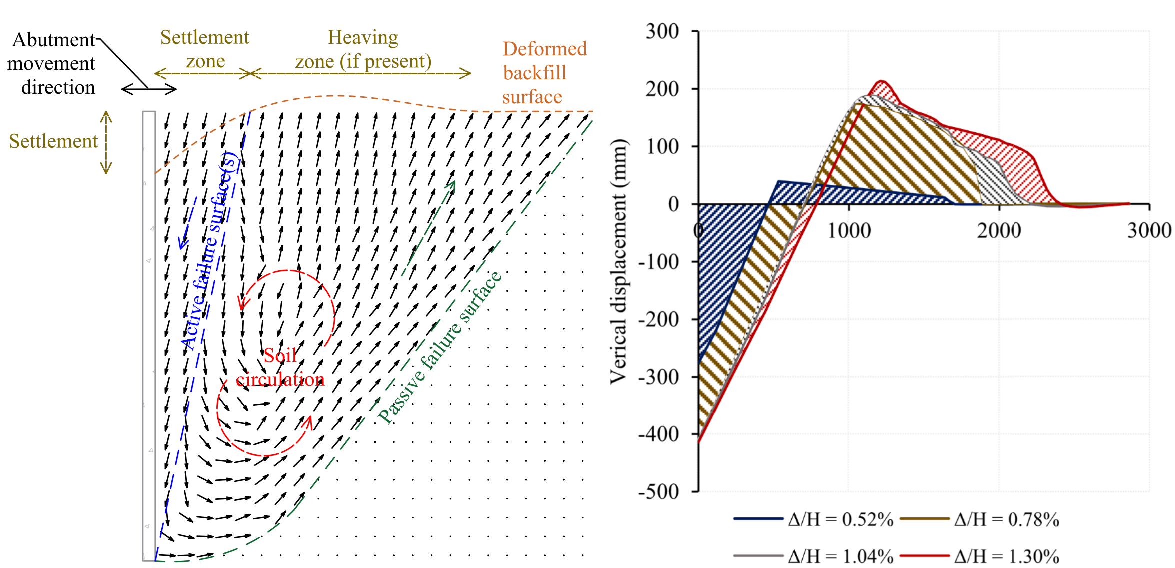

(a) *(b)*

Fig. 5. (a) Schematic of backfill direction vectors for a normalized abutment movement displacement of 1.30% (reproduced from Sigdel et al. [108]) and (b) Backfill profile after 120 cycles for various abutment movement amplitudes (reproduced from Sigdel et al. [108]).

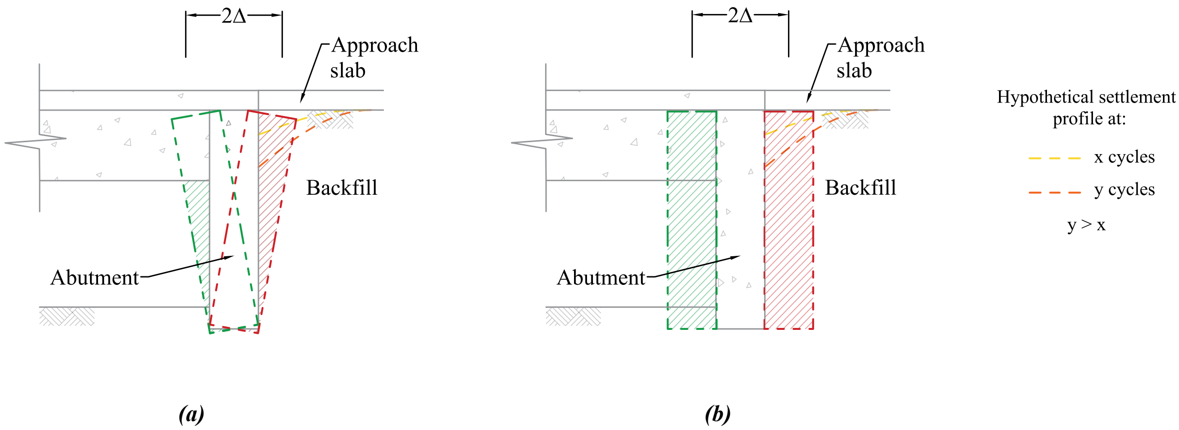

Fig. 6. Idealized movement modes of integral abutments:(a) rotational and (b) translational.

characteristics typically observed in denser soils. However, from a review of experimental data in available literature, this statement cannot be corroborated as there is considerable variation in the observed responses. For instance, in investigations carried out by Zadehmohamad et al. [140] and Havinga et al. [39], involving backfills with respective relative densities of 85 % and 58 %, considerable soil upheaving was observed. However, in the works of Morley et al. [89], Liu et al. [70] and Ng et al. [92], involving backfills with relative densities of up to 85 %, heaving was not reported. It is believed that this variation is due to the dependency of the backfill deformation on other loading conditions such as abutment displacement magnitude, height of the retained fill and abutment movement mode. Further, dilatancy characteristics are also highly influenced by the microscopic characteristics (such as particle shape) of the soil itself [132]. Moreover, the backfill of small-scale IAB models are also subjected to smaller confining pressures, which in turn results in an exaggerated dilative response [79]. Hence, deriving generalized relationships can be challenging, which may also signify as to why research outcomes on the soil deformation response of integral bridges is limited relative to that on lateral stress ratcheting. As such, further experimentation, using large-scale physical models, while considering a wide range of relative densities and with a backfill soil typically used in field IABs (such as well/uniformly graded gravel [41]), would be beneficial in improving the understanding of this aspect.

Regardless, a deduction on the potential mechanism of the soil-structure interaction of integral bridges can be made from an evaluation of the results of Sigdel et al. [108]. In many instances, research has often solely attributed the escalation of lateral stresses acting on integral abutments to the progressive densification that occurs as a result of the cyclic active failures and subsequent compressive strains experienced by the backfill (e.g., Alqarawi et al. [7], Khasawneh [53]). However, through large-scale physical modelling, Sigdel et al. [108] observed that despite settlements reaching almost stable conditions, soil upheaval continues to propagate. This can be visualized in Fig. 5 (b) which has been generated based on the experimental data of Sigdel et al. [108]. The illustration is comprised of the backfill profiles after 120 cycles of varying abutment amplitudes, along with shaded regions which represent the corresponding settlement troughs and upheaved soil. Here, it is evident that with increasing displacements, the overall volumetric response seems to change from contractive to slightly dilative, with the trials of $\Delta/H = 1.04$ % and $\Delta/H = 1.30$ % exhibiting net volumetric strains of −0.19 % and −0.83 %, respectively. This is indicative that soil densification is not the sole occurring mechanism. Sigdel et al. [108], through a PIV analysis, noted that this was caused by a 'circulation' of soil particles. This observation has been illustrated by the red arrows in Fig. 5 (a). It is postulated that this is a depiction of changes to the soil fabric, wherein the granular particles experience rolling during active wall movement, resulting in a development of the network of granular particles. Similar observations were previously made in investigations involving radial (lateral) cyclic triaxial testing on granular specimens [134,135,24,133]. This postulation also provides a possible explanation as to why longer integral bridges are subjected to greater magnitudes of stress ratcheting. Moreover, these results also pose added concerns for approach slabs used with longer IABs, as greater heaving would correspond to larger hogging flexural strains.

Impact of abutment movement mode on soil-structure interaction

Relationship between abutment movement mode and lateral pressure ratcheting

Centrifuge data from Springman et al. [113], along with field observations, such as those reported in Lawver et al. [65] and Darley et al. [27], have indicated that the movement of integral abutments vary between translational and rotational modes (refer Fig. 6). The degree of either movement mode has been found to depend on factors such as abutment type, abutment geometry, foundation design and properties of the surrounding soil [128,47]. Classical earth pressure theories, however, such as those of Coulomb [26] and Rankine [100], compute pressure magnitudes assuming that the retained soil is at a state of passive (or active) failure, with horizontal pressures varying linearly with height, independent of the type and extent of the abutment movement.

To assess the impact of the abutment movement mode on the soil-structure interaction response, Alqarawi et al. [7] conducted a comparative study using a large-scale (1:2 scale) physical model of an integral abutment. A translational movement of a given amplitude would theoretically impart twice the volumetric strain on the backfill relative to that of a rotational movement of equivalent displacement. Hence, evaluations in this study were made considering translational perturbations with displacement magnitudes 50 % of that of the rotational cases [7]. Despite this, as illustrated by the graphs in Fig. 7 (refer data specific to cases Alq-Rot and Alq-Trans), the translational movements resulted in notably greater peak pressures, with a percentage difference of up to approximately 84 %.

Apart from variations in lateral stress magnitudes, the abutment movement mode also impacts the pressure profile along the abutment height. The plot in Fig. 7 includes other lateral pressure data from the following selected literature: Luo et al. [78], Sigdel et al. [108], Luo et al. [77], Zadehmohamad et al. [140], Lehane [66] and England [32]. From the figure, it is apparent that rotational abutment movements (dashed lines) typically lead to peak pressures near the mid-height of the abutment, dropping to relatively insignificant values near the abutment toe. Conversely, translational abutment movements (solid lines)

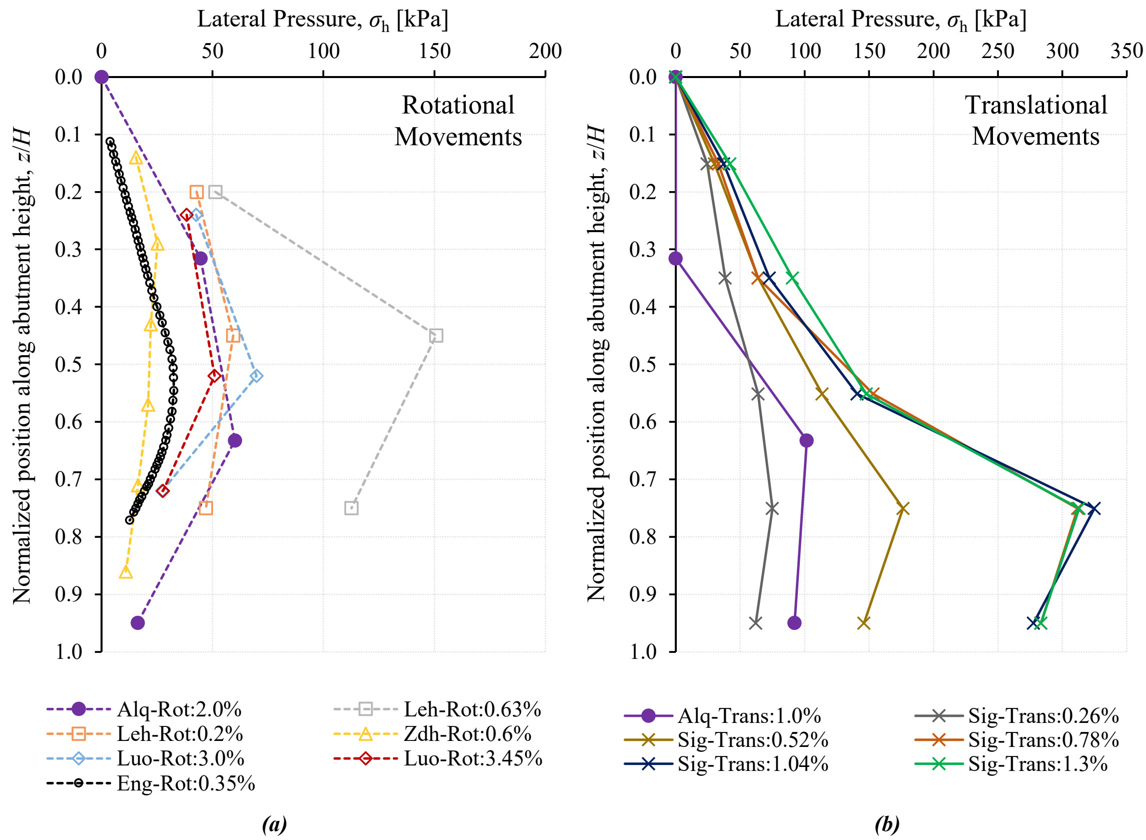

Fig. 7. Lateral pressure profile results from (a) rotational and (b) translational abutment movements (reproduced from selected experimental and numerical studies).

generate the highest pressures closer to the base of the abutment. Similar observations were noted from numerous experimental and numerical studies, such as those by Liu et al. [72], Liu et al. [74] and Zadehmohamad and Bazaz [139]. The differences in lateral pressure distributions for these abutment movement types indicate that soil arching is taking place [92]. This can be better understood by referring to Fig. 6. In the case of rotational abutment movements, strains are imposed on the backfill primarily at the upper region, with the soil closer to the abutment toe receiving little to no disturbance. Hence, in such scenarios, soil stiffening predominately takes place in the upper region of the backfill. However, as the number of applied cycles increase and the corresponding settlement trough adjacent to the abutment develops (refer legend of Fig. 6), the backfill in the upper region is subjected to increasingly less shear strains. Pure translational movements, however, impart constant (ideally) compressive strains along the full height of the abutment, thus the lower regions of the backfill experience sustained densification effects with each cycle. This addresses as to why stress accumulation is more critical in the case of translational abutment movements.

Effect of foundation design option on lateral pressure ratcheting and soil deformation

While the observations in Sec. 4.1 highlight the significance of the abutment movement mode and may suggest that translational movements are critical to IAB design, it is crucial to consider these movement types from a practical perspective. From field observations of integral bridges, it has been determined that the mode of the abutment movement is of a composite nature, wherein both abutment translation and rotation occur simultaneously [65,27]. The degree of either movement type has been observed to be dependent on factors such as abutment geometry and restraint imposed by the foundation design (foundation stiffness) [47]. Moreover, in certain legislative guidelines, integral bridges are subcategorized based on the foundation configuration. For instance, in the UK, there are 6 types of integral abutments, such as frame abutments (refer Fig. 8 (a) and (b)), bank pad abutments and embedded wall abutments (refer Fig. 8 (c)) [16]. And herein, the methodology to predict passive lateral stresses due to thermal movements vary based on the type of integral abutment. Despite this, while notable research efforts have been made towards understanding the soil-pile interaction of integral bridges (e.g., Alshawabkeh and Issa [8], Tabatabai et al. [115], Huang et al. [45]), investigations on the impact of foundation design on the IAB backfill-abutment interaction is very limited.

For example, through a field instrumentation of 4 IABs, Kim and Laman [57] observed that longer (slender) abutments typically experience greater magnitudes of abutment rotation, while shorter abutments (e.g., semi-integral abutments) exhibit translational dominant movement. Concurrent observations were made by Civjan et al. [23], where field instrumentation data of two IABs, each supported on 4 m high abutments that are in turn founded on 5 steel H-piles oriented for weak-axis bending (web is perpendicular to the centerline of the bridge) have been reported. Here, due to the flexible foundation but moderately large abutment height, the abutment primarily experienced rotational movements with the abutment top having displacements two–three times greater than that of the abutment toe. Hence, while outcomes from analyses involving pure rotational/translational movements are beneficial in developing the understanding of the backfill-abutment interaction, it would be inappropriate to use such data as a means of predicting field behavior.

In majority, experimental research of integral bridges, such as that by Tapper and Lehane [117], Duda and Siwowski [30] and Makino et al. [81], has involved the utilization of models where movement is assumed to be one of the two idealized cases. This is potentially due to the added complexity and expenditure that would be involved with incorporating a foundation into the model. Some preliminary attempts, however, have

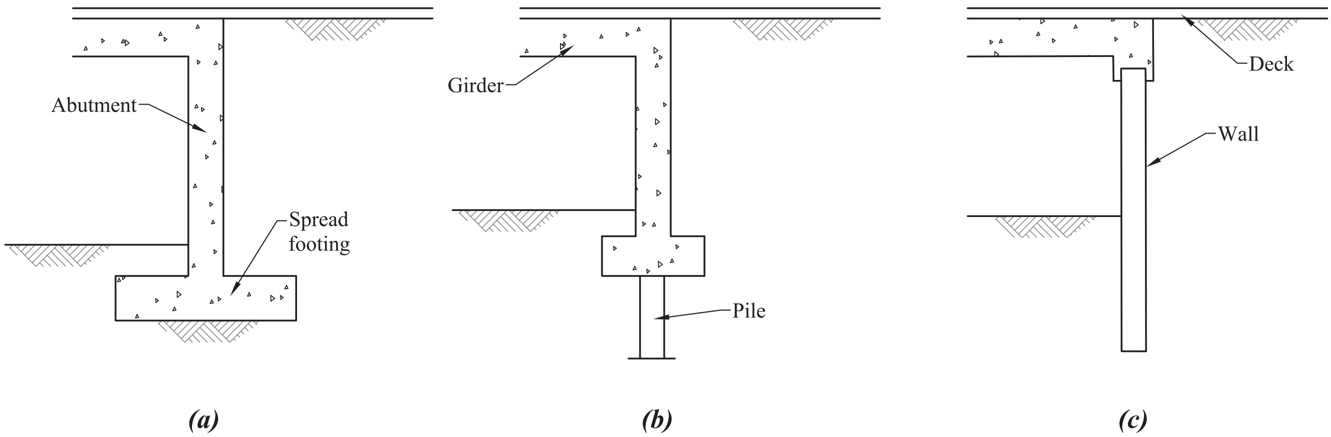

Fig. 8. Examples of IAB foundation configurations (reproduced from BSI [16]).

been made to assess the impact of foundation stiffness on the abutment behavior. Using finite element analyses, Abdullah and El Naggar [3] observed that using a larger pile section resulted in decreased lateral pressures acting on the abutment. A similar response was noted when switching the pile orientation from weak-axis to strong-axis bending. Herein, this behavior was attributed to the concept of force equilibrium, whereby greater pile inertia would lead to a greater distribution of lateral loads to the piles. These observations, however, contradict the findings of Liu et al. [72], where an increase in foundation rigidity corresponded to greater passive pressures across the full height of the abutment. While the exact cause for this disparity is not yet completely understood, a contributing factor is the modelling assumption of the abutment-foundation connection. Liu et al. [72] utilized a pinned connection whereas Abdullah and El Naggar [3] adopted a fixed connection. The work of Abdel-Fattah and Abdel-Fattah [2] provided some additional insights by numerically comparing the lateral pressure response for a framed integral abutment on a spread-base footing to that of a piled abutment. Here, for both foundation options, a similar pressure profile was obtained in the upper half of the abutment wall. The piled foundation, however, resulted in notably larger lateral pressures near the base of the abutment. This response is potentially because the spread-base footing provided greater restraint to abutment toe movement, thus reducing the lateral stresses induced near the base of the abutment. A recent investigation by Morley et al. [88] involved the use of a centrifuge to assess the SSI behavior of a frame abutment with a spread footing (refer Fig. 8 (a)). Herein, for all trials, peak passive pressures occurred at $0.3 < z/H < 0.5$, dropping to considerably smaller magnitudes towards the lower region of the abutment. This overall lateral stress profile is expected for abutments with rotationally dominant movements, albeit with a somewhat higher maximum pressure location. This difference in peak pressure location could originate from the height of the abutment [128], which for the centrifuge model was 9 m, while the cases presented in Fig. 8 (b) have a maximum retained height of 4 m. Regardless, the work of Morley et al. [88] highlights the importance of considering the actual boundary conditions of the foundation during the design of IABs. However, these studies are yet inadequate to understand the long-term impact of foundation choice on the lateral stress ratcheting phenomenon. While there are several published reports on field monitoring data of integral bridges supported on various foundation types, attempting to make direct comparisons between the observed lateral pressure responses would be inappropriate. This is because, as highlighted in Sec. 2.2, field bridges are subjected to site-specific conditions that influence the SSI behavior.

There is a sparsity of research available on the discussion of the impact of foundation design on soil deformation occurring in integral bridge approach backfills. Via finite element analyses, Liu et al. [72] noted that the footing stiffness has a negligible effect on the settlement profile. Through the use of a small-scale physical model, Liu et al. [70], however, observed that the footing rigidity influences the displacement of the abutment toe which in turn affects settlement magnitudes to a notable degree. Specifically, during the passive phase of the abutment movement, the abutment with the less rigid foundation experienced greater toe movements away from the backfill. After 30 loading cycles, the abutment with a more rigid footing exhibited a maximum settlement 22.1 % greater relative to that in the case involving an abutment with the more flexible foundation[70]. This result is counterintuitive as greater toe movement implies greater allowance for soil slumping which in turn would result in larger subsidence at the bridge approach. However, despite these contradictions, these observations not only highlight the potential significance of foundation design on progressive soil deformation occurring in IABs, but also reiterates the importance of modelling assumptions on the observed response. Hence, there is a clear requirement to assess the impact of various foundation design options, coupled with a range of abutment heights, on the abutment movement mode, and its corresponding implications on the long-term behavior of integral abutment bridges.

Impact of bridge skew on the lateral pressure response

Bridge skew is a parameter that is stringently restricted in most (if not all) legislative guidelines on the design of integral bridges. For example, in the USA, the maximum skew limit varies from 0° to 60°, depending on the state in consideration, integral bridge type (semi or full), bridge length and foundation design choice [50,105,49]. Here, maximum allowable skew angle typically has a negative correlation with maximum allowable bridge length. This is due to the observations made from previous investigations that have led to the understanding that skew angles result in more critical passive lateral earth pressures at the obtuse corners of the bridge [104,31]. Through field monitoring of two integral bridges, Civjan et al. [23] noted that a bridge with a 15° skew exhibits maximum lateral earth pressures more than double of that experienced by a straight bridge. A corresponding determination was also made by Frosch and Lovell [35]. Similar observations have also been made for a curved integral bridge. Through a 1-year field monitoring effort of a 69 m long IAB with a curvature of 27°, it was noted that the obtuse corner of the abutment experienced a greater rise in lateral pressures during the positive temperature differential phase [10]. This transverse variation of lateral stresses across the abutment wall is due to the anti-symmetric geometry of skewed bridges, which apart from longitudinal deformations during thermal loading, also induces bidirectional bending and torsion [61]. Concurrent determinations have been made through field instrumentation data presented in Bahjat [11], Khodair and Hassiotis [55] and Kirupakaran et al. [59].

Additional insights, however, have been presented in a relatively recent study by Khasawneh [53], which involve the use of both experimental (small and large-scale) and numerical methods (utilizing proposed constitutive relations based on the experimental data). As depicted in Fig. 9 (a), for a skew angle of 60°, the critical passive pressures at the obtuse corner seem to only act on a small region across the abutment width [53]. This differs to the idealized pressure distribution proposed in [17], wherein lateral pressure is assumed to increase linearly from the acute corner to the obtuse corner [51]. A comparison between the observed and assumed pressure distribution (using hypothetical pressure coefficient values) has been included in Fig. 9 (a). This juxtaposition is crucial as it indicates that the bending moments based on the idealized pressure distribution would be significantly greater than that from Khasawneh [53]. Consequently, this can lead to conservative integral abutment design.

It was also determined that while larger skew angles result in greater total abutment deformations, the peak passive pressures decrease [53]. This is because, as indicated in Fig. 9 (b), larger skew angles were observed to result in a larger component of transverse displacement, but a smaller longitudinal deformation constituent. Collectively, these findings on the behavior of skewed bridges provide an alternative perspective, which may potentially allow for the relaxation of the skew limits on integral bridges. However, the methodology of the investigation does possess certain limitations that should be addressed. The constitutive model used in Khasawneh [53] was developed and calibrated against experimental data wherein the confining pressures are considerably lower (backfill retention height of 0.30 m) than that of a typical field IAB. Further, only ten annual thermal cycles were considered, which is notably less than that in the design life span of integral bridges. Hence, it would be of value to comprehensively study the effects of increasing bridge skew angle on the longitudinal deformation of the abutment, along with the corresponding implications on the lateral pressure response of integral bridges. This would allow for a corroboration and sound conclusion of these observations.

Approaches to alleviate the temperature-induced SSI effects

To reduce the thermally induced adverse SSI effects on integral bridge approaches, considerable investigations ranging from numerical analyses to full-scale testing have been performed. These methods can be classified to two broad categories: compressible inclusions (refer Fig. 10 (a)) and mechanically stabilized earth (MSE) systems (refer Fig. 10 (b)). The former involves placing a highly elastic layer in between the abutment and backfill, while the latter utilizes geosynthetics to reinforce the retained soil mass. It should be noted that approach slabs (e.g., Liu et al. [68],Dreier et al. [29]) have been excluded from the following discussion as the strategies are limited to those that reduce the accumulation of passive lateral pressures and backfill deformations.

The performance of compressible inclusions in integral bridge approaches have been explored over the last two decades, with expanded polystyrene (EPS) geofoam being the material of choice. Using numerical analysis, Horvath [43] evaluated the performance of EPS in a 6 m high IAB model. Here, after 4 thermal cycles, use of a 100 mm isolation block resulted in considerable reductions in passive lateral pressures across the entire height of the abutment, with peak pressures minimized by 57.8%. This observation has been corroborated by subsequent scaled physical model tests conducted by Alqarawi et al. [7], involving trials with up to 20 cycles. Additional insights on the performance of EPS were provided by the numerical works of Liu et al. [76], Burugupelly and Dasaka [18] and Al-Qarawi et al. [9]. Herein, two key relationships were determined: (1) lateral pressures have a positive correlation with the elastic modulus of EPS and (2) lateral pressures exhibit a negative correlation with inclusion thickness. This behaviour of EPS (or any other compressible inclusion material) can be explained through Eqn. (2), which can be termed as 'transfer function' of an inclusion. It is a simplified derivation, assuming stress equilibrium between the compressible inclusion and backfill soil, along with a purely elastic inclusion material. Therein, $\boldsymbol{\varepsilon}_{soil}$ is the strain experienced by the soil, $\mathbf{E}_r$ is the relative stiffness which is a function of the stiffness of soil $\mathbf{E}_{soil}$ and inclusion $\mathbf{E}_{inc.}$, Δ is the abutment displacement and t_{inc} is the thickness of the inclusion layer. Through this, it can be understood that an inclusion decreases the imposed displacements on the retained soil, and hence, reduces the stress ratcheting effect. Further, the expression also indicates that an inclusion with a smaller elastic stiffness and/or greater thickness will yield further reductions to the strains imposed on the backfill. A recent study by Sigdel et al. [108] assessed the capabilities of an alternative inclusion material, namely expanded thermoplastic polyurethane (E-TPU). Herein, for the same inclusion thickness, it was observed that the E-TPU inclusion yielded a further 47.1% decrease in peak lateral stresses when compared to EPS. The difference in response can be attributed to the elastic modulus of the utilized E-TPU grade, which was 435 kPa. This is around 10.5 times smaller than that of the used EPS grade. Duda and Siwowski [30] utilized a full-scale physical

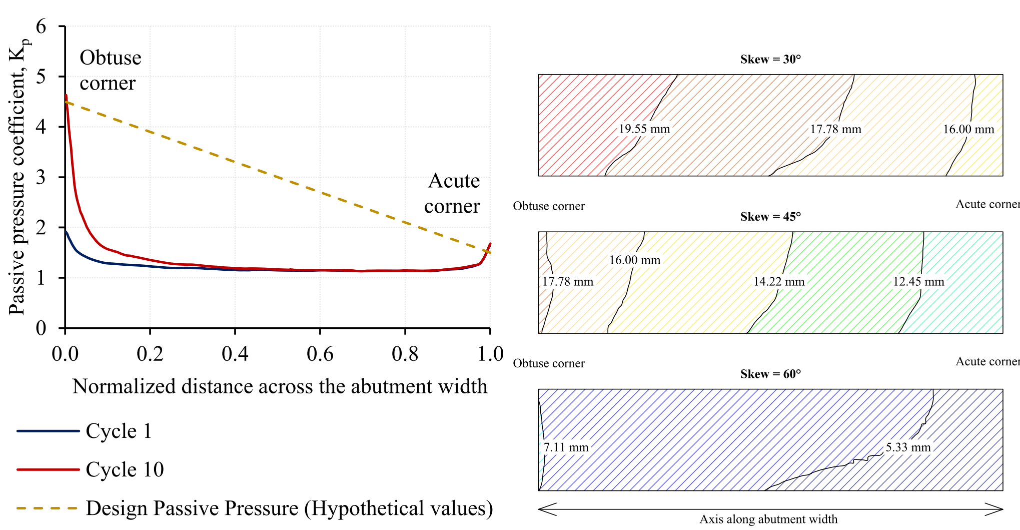

(a) *(b)*

Fig. 9. (a) Transverse distribution of passive lateral pressure coefficient for integral bridge with a 60° skew (reproduced from Khasawneh [53]) and (b) variation of longitudinal displacement across the abutment width with increasing bridge skew (reproduced from Khasawneh [53]).

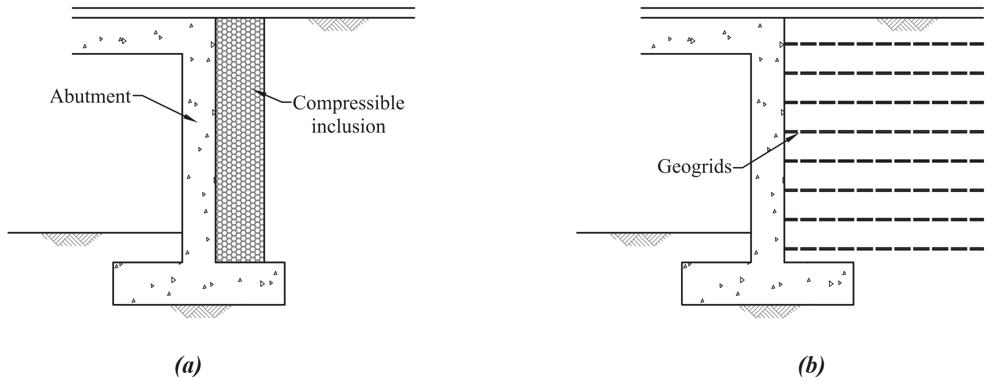

Fig. 10. Schematic of an IAB with (a) compressible inclusion and (b) mechanically stabilized earth system.

model to evaluate the performance of recycled tyre bales interspersed with sand, along with a layer of tire-derived aggregates (TDA) directly adjacent to the abutment wall, in reducing the SSI effects of integral bridge approaches. Herein, after at least 2500 loading cycles, the composite backfill yielded notably smaller passive pressures when compared to theoretical pressures for a typical granular backfill. Through small-scale experiments, Zadehmohamad et al. [140] evaluated the performance of a 150 mm thick tire-soil layer as a compressible inclusion. It was observed that the layer reduced the long-term passive pressure coefficient by 25.9 %, with the improvements increasing with the proportion of tire particles in the inclusion layer.

$$\boldsymbol{\varepsilon}_{\text{soil}} = \mathbf{E}_{\text{r}}\frac{\Delta}{t_{\text{inc.}}};\quad \text{where}\ \ \mathbf{E}_{\text{r}} = \frac{\mathbf{E}_{\text{inc.}}}{\mathbf{E}_{\text{soil}}} \tag{2}$$

The benefits of compressible inclusions have also been validated in the field. Hoppe [42] presented instrumentation data from a 100 m semi-integral abutment bridge, with a 250 mm thick EPS pad. Herein, throughout a 5-year monitoring period, considerable decreases in passive lateral pressures were noted. Moreover, design guidelines such as the Pennsylvania Department of Transportation Design Manual [95] and Virginia Department of Transportation Manual of the Structure and Bridge Division [124] have included EPS in the design recommendations. However, while the above points highlight the benefits of compressible inclusions, some critical limitations should be addressed. All the experimental studies assessing the capabilities of inclusions utilize loading rates significantly higher than the one-year time period of seasonal thermal cycles. And due to the visco-elasto-plastic properties of EPS [120], these higher loading rates could lead to higher estimated yield stresses, and smaller accumulations of plastic strains in the inclusion. Collectively, this can result in overestimations in the inclusion performance. Also, the constitutive relations used by Horvath [43], Al-Qarawi et al. [9], Burugupelly and Dasaka [18] and Liu et al. [76] to numerically simulate the behaviour of EPS have not been appropriately validated against cyclic element tests conducted on the material. Hence, it is suggested that future investigations into compressible inclusions utilize appropriate means to account for the rate-dependency and cyclic response of EPS to quantify the ideal thicknesses for a range of integral bridge lengths. The authors are currently developing a methodology for this.

Investigations assessing the performance of compressible inclusions against the progressive backfill deformation phenomena of IAB approaches is limited. It has been determined that during the active phase of the abutment, the compressible inclusion is displaced due to the active pressure of the retained soil [7]. This causes the backfill to experience soil slumping, albeit to a lesser extent when compared to a soil-only backfill. Al-Qarawi et al. [9] observed that backfill deformations could be further reduced by increasing the thickness of the inclusion, and this response is understood through Eqn. (2). While the above aims to reduce backfill settlements through the minimization of the transfer of displacements through the inclusion, another approach has been to increase the safety factor of the backfill against slope failure. Al-Qarawi et al. [9] and Horvath [43] investigated the effectiveness of using a wedge-shaped inclusion arrangement over a typical rectangular block. The former noted that the wedge shape inclusion resulted in a 16.2 % decrease in settlements after 30 cycles. Despite this improved performance, the settlement at the end of the trial was 26.2 mm which equates to a normalized settlement $s/H = 0.11$ (normalized against backfill height, H), which is still an undesirable magnitude. This is a common issue noted by other investigations such as Alqarawi et al. [7], Sigdel et al. (2023) and Liu et al. [76]. Hence, it is the authors' belief that a compressible inclusion by itself is an incomplete solution and should be used in tandem with other methods to improve the stability of the retained soil.

Another widely researched option involves creating a self-stable approach backfill using geosynthetic reinforcement [43]. Thorough reviews on the performance of mechanically stabilized earth (MSE) systems in integral bridge approaches have been carried out by Liu et al. [75] and Tatsuoka et al. [119]. Hence, this current study will only briefly summarize previous observations and will instead focus on the developments not highlighted by the aforementioned articles. When considering the performance of MSE systems in minimizing the ratcheting of passive lateral pressures, studies have reported conflicting observations. Through small-scale physical modelling, Tatsuoka et al. [118] observed that use of geogrids resulted in larger passive pressures when compared to an unreinforced backfill. Similar reports have been made in more recent studies by Liu et al. [71]. However, through experimental means, Farhangi et al. [33] demonstrated that the MSE backfill exhibited a smaller lateral pressure coefficient when compared to the control experiment. Zadehmohamad and Bazaz [139] experimentally investigated the performance of geocells. Here, after 120 cycles, the passive pressure coefficient for the geocell reinforced and unreinforced backfills was 4.8 and 6.8, respectively. Further, reductions in lateral pressures exhibited a strong positive correlation with geocell length. Liu et al. [76] assessed various geogrid configurations such as the connection of geogrid to the abutment wall, facing type, length and spacing of the geogrids. Herein, after 5 cycles, use of wrap-around geogrids yielded a 6.6 % decrease in peak pressures relative to the unreinforced backfill. However, all other MSE configurations resulted in an almost identical lateral pressure distribution. Therefore, the suitability of using geosynthetic reinforcements in IAB approaches to reduce long-term lateral pressures is inconclusive.

Observations regarding the performance of MSE backfills in attenuating progressive backfill deformations in integral bridge approaches are more unified. Through experimental investigations, Liu et al. [71] observed that use of straight unconnected geogrids resulted in greater maximum settlements, but a smaller zone of influence. Herein, however, geogrids with a wrap-around facing yielded minor reductions in maximum settlement when compared to the control case. In both cases, use of geosynthetics reduced the volume of soil slumping. Similar findings were reported by Liu et al. [74]. Tatsuoka et al. [118] compared the capabilities of connected and unconnected geogrids in a small-scale IAB model. For a trial involving only active-neutral cycles of $\Delta/H = 0.2$ %, the unreinforced backfill exhibited a normalized settlement $s/H = 1.67$ %, while that for the backfills with unconnected and connected geogrids were $s/H = 0.80$ % and 0.06 %, respectively. Concurrent observations regarding connected geogrids were presented in Farhangi et al. [33]. In an unreinforced IAB approach backfill, the retained soil experiences slope failure during the active phase of the abutment movement, which over the course of 120 cycles results in notable deformations. The presence of geogrids in the backfill increase the stability of the soil mass, reducing the extent of soil slumping, thus minimizing settlements.

To maximize the benefits brought by both compressible inclusions and MSE backfills, preliminary research efforts have been made to assess the response of a combined system incorporating both methods. Mitoulis et al. [84] assessed the benefits of geogrids coupled with a TDA compressible inclusion using finite element analysis. After ten thermal cycles, the combined system resulted in significantly larger improvements to peak passive pressures when compared to the MSE-only and unreinforced backfills. Similar observations against backfill deformations were also reported. A subsequent study by Caristo et al. [19] extended this work by investigating a similar inclusion-MSE backfill for 120 cycles. At the conclusion of the analysis, the combined system resulted in considerable reductions to both passive pressures and backfill deformations, with peak lateral stresses decreased by 89.8 %. However, the aforementioned two studies utilized the Mohr-Coulomb constitutive model to simulate the soil behavior, which has been reported to be an inappropriate choice to model the cyclic response of IAB approaches [37]. The performance of a combined inclusion-MSE backfill was also numerically evaluated by Liu et al. [76]. However, given that the lateral pressure results of only the first passive phase were discussed in this study, the cyclic performance of this system is inconclusive. Through small-scale experiments, Liu et al. [71] reported interesting findings regarding the capabilities of a inclusion-MSE backfill. The combined system resulted in smaller passive pressures during the first cycle, but greater ratcheting effects in subsequent cycles. This led to more critical peak pressures at cycle 30 when compared to an unreinforced backfill and backfill with only geogrids. This observation is counterintuitive as the reason for attempting the combined inclusion-MSE system was due to the capabilities of compressible inclusions in minimizing the development of lateral stresses. Regardless, the inclusion-MSE backfill reduced deformations to a greater extent when compared to a MSE-only and an inclusion-only backfill [71]. Collectively, due to the limitations in the methodologies of the above numerical works, along with constraints imposed by small-scale modelling, it is important to further explore the concept of compressible inclusion-MSE backfills.

Conclusions

Integral bridges are a relatively recent design concept in which there is structural continuity between the girders and abutments, leading to numerous economic and performance benefits. However, this connection has resulted in a transference of longitudinal deformations from the superstructure to the substructure, ensuing a complex cyclic interaction with the surrounding soils. This has resulted in geometric limitations, inhibiting the potential of this concept, and thus making it a topic of interest amongst the research community. An analysis of contemporary literature has highlighted the following:

- The long-term lateral stress ratcheting response is highly dependent on the magnitude of abutment displacement, which is in turn primarily governed by the bridge length. With increasing abutment displacements, the degree of stress accumulation with each loading cycle rises. Additionally, the number of cycles required to reach a limiting state of passive pressure escalation has a positive correlation with the displacement amplitude, indicating that during the design of longer integral bridges, an analysis considering the full lifespan of the structure is required. Hence, it is suggested that future analyses consider the number of annual cycles equivalent to the design life of IABs to understand the critical loading conditions.
- In countries such as the UK, Australia and New Zealand, the analytical models provided in legislative guidelines for integral bridge design are unable to reasonably estimate the peak passive pressure magnitudes for a wide range of bridge lengths. In other regions, engineers typically use empirical knowledge or refer to earth pressure theories based on monotonic loading conditions, which may lead to uneconomical design of these structures.
- The monitoring period of field instrumentation of bridges available thus far is insufficient to make any concrete conclusions on the long-term lateral pressure response. This is particularly true for longer IABs, given the determined relationship between abutment displacement and stress ratcheting. Regardless, it is evident that the lateral stress escalation observed from controlled analyses are low relative to that exhibited by the field bridges. This is primarily due to the assumption that longitudinal deformation is unrestrained and uniform throughout the superstructure cross section. As such, upcoming investigations should consider the effects from factors such as backfill restraint, superstructure geometry, construction material and solar radiation on the abutment displacement magnitude, as it would yield modelling results that better correspond to field behavior.
- Soil deformation in integral bridge approach backfills consist of soil subsidence and upheaving. The former exhibits similar behavioral trends to lateral stress escalation. The presence of the latter, however, seems to be dependent on several factors such as magnitude of abutment displacement, mode of abutment movement, stress state and dilatancy properties of the soil. Hence, it is recommended that future studies carry out experimental/numerical analyses at field stress conditions and adopt a backfill material typically used in industrial practice.
- With increasing abutment displacement, despite soil settlement reaching stable conditions, upheaving continues to progress, resulting in a net dilative volumetric response. This is indicative that the backfill-abutment interaction of IABs involve not only densification, but also fabric development. As such, when utilizing numerical analysis tools, it is imperative to employ constitutive relations that can capture these effects.
- The degree of rotation and translation in the displacement of integral abutments significantly influences the lateral pressure response of integral bridges. Due to soil arching, rotationally dominant abutment movement results in stress accumulation primarily along the upper half of the abutment wall, whereas translational movements induce critical passive pressures closer to the abutment toe. Additionally, translational abutment movements lead to relatively greater magnitudes of stress escalation.
- Some preliminary attempts have been made to investigate the impact of foundation restraint on the backfill-abutment interaction of IABs. However, to knowledge, there is still limited research that has assessed the influence of various foundation configurations on the abutment movement and corresponding long-term effect on the lateral stress ratcheting and soil deformation phenomena. As such, it is recommended that future studies consider the proper boundary conditions of various foundation designs. This would allow for the development of analytical models for the estimation of lateral pressure accumulation and soil subsidence under a variety of loading conditions.
- As a result of previous investigations on the relationship between bridge skew and lateral pressure, a skew angle limit is explicitly defined in a majority of design guidelines on integral bridges. A more

recent study, however, indicates that increasing bridge skew angles have an inverse correlation with abutment longitudinal deformation, and consequently with passive lateral pressures. However, due to methodological limitations of this particular study, further examination on this interdependence is required.

- Compressible inclusions have demonstrated the ability to minimize the transfer of thermal displacements to the backfill. However, the utilized constitutive models do not account for the cyclic characteristics of the compressible material. Further, experimental models typically use loading rates considerably higher than the one-year time period of annual cycles, which can lead to an overestimation in performance. Hence, it is recommended that future investigations account for these characteristics to provide accurate estimations of compressible inclusion behavior in integral bridge approaches.
- Combined inclusion-MSE backfills have been demonstrated to be very effective in attenuating the development of permanent deformations in the backfill. However, the performance of the combined backfill system against the ratcheting of passive lateral pressures is still uncertain due to conflicting observations. Moreover, most constitutive models utilized to simulate the backfill behavior in numerical investigations do not adequately account for the cyclic attributes of granular soils. As such, it would be of value to utilize modern constitutive formulations in finite element analyses to study the long-term benefits of combined inclusion-MSE backfills.

CRediT authorship contribution statement

M.S.K. Hassan: Investigation, Formal analysis and Writing – original draft. **D.S. Liyanapathirana:** Writing – review & editing, Supervision, Project administration. **W. Fuentes:** Writing – review & editing, Supervision. **C.J. Leo:** Writing – review & editing. **P. Hu:** Writing – review & editing.

Declaration of competing interest

The authors declare that they have no known competing financial interests or personal relationships that could have appeared to influence the work reported in this paper.

Data availability

The authors do not have permission to share data.

Acknowledgements

This investigation was supported under the International Postgraduate Scholarship provided by Western Sydney University.

References

[1] Abasi A, Shid-Moosavi S, Rahai A. Seismic performance of integral, semi-integral, and conventional bridges. In: 5th International Conference on Bridges, Tehran, Iran; 2019. https://www.researchgate.net/publication/341909051_Seismic_Performance_of_Integral_Semi-Integral_and_Conventional_Bridges.

[2] Abdel-Fattah MT, Abdel-Fattah TT. Behavior of integral frame abutment bridges due to cyclic thermal loading: nonlinear finite-element analysis. J Bridg Eng 2019;24(5):04019031. https://doi.org/10.1061/(ASCE)BE.1943-5592.0001394.

[3] Abdullah A, El Naggar H. Soil-structure interaction of integral abutments. Transp Geotech 2023;38:100900. https://doi.org/10.1016/j.trgeo.2022.100900.

[4] Abendroth RE, Greimann LF, LaViolette MD. An integral abutment bridge with precast concrete piles (TR-438); 2007. https://intrans.iastate.edu/research/completed/an-integral-abutment-bridge-with-precast-concrete-piles-tr-438/.

[5] Abid SR, Tayşi N, Özakça M. Experimental analysis of temperature gradients in concrete box-girders. Constr Build Mater 2016;106:523–32. https://doi.org/10.1016/j.conbuildmat.2015.12.144.

[6] Aktan H, Attanayake U, Ulku E. Combining link slab, deck sliding over backwall, and revising bearings (RC-1514); 2008. https://rosap.ntl.bts.gov/view/dot/39516.

[7] Alqarawi AS, Leo CJ, Liyanapathirana DS, Hu P. Soil-structure interaction issues in integral abutment bridges. Transp Geotech 2024;48:101296. https://doi.org/10.1016/j.trgeo.2024.101296.

[8] Alshawabkeh YM, Issa MA. Maximum permissible safe length of integral abutment bridges supported by steel H-Piles. Structures 2024;62:106130. https://doi.org/10.1016/j.istruc.2024.106130.

[9] Al-Qarawi AS, Leo CJ, Liyanapathirana DS. Effects of wall movements on performance of integral abutment bridges. Int J Geomech 2020;20(2):04019157. https://doi.org/10.1061/(ASCE)GM.1943-5622.0001559.

[10] Alhowaidi Y, Kim S, Eun J. Field monitoring of soil response for curved integral abutment bridge during seasonal temperature changes. Geo-Congress 2023, Los Angeles, California; 2023. 10.1061/9780784484685.042.

[11] Bahjat R. Short and long-term performance of a skewed integral abutment prestressed concrete bridge UMass Amherst]; 2014. 10.7275/5785180.

[12] Banks, J. R. & Bloodworth, A. G. (2018). Lateral Stress Profiles on Integral Bridge Abutments. Proceedings of the Institution of Civil Engineers - Bridge Engineering, 171(3), 155-168. 10.1680/jbren.17.00017.

[13] Bonczar, C. H., Brena, S. F., Civjan, S. A., DeJong, J. T., Crellin, B. J., & Crovo, D. S. (2005). Field Data and Fem Modeling of the Orange-Wendell Bridge. Integral Abutment and Jointless Bridges (IAJB 2005), Baltimore Maryland, United States. https://trid.trb.org/view/850769.

[14] Breña SF, Bonczar CH, Civjan SA, DeJong JT, Crovo DS. Evaluation of seasonal and yearly behavior of an integral abutment bridge. J Bridg Eng 2007;12(3):296–305. https://doi:10.1061/(ASCE)1084-0702(2007)12:3(296).

[15] Briseghella B, Zordan T. An innovative steel-concrete joint for integral abutment bridges. J Traffic Transport Eng (Engl Ed) 2015;2(4):209–22. https://doi.org/10.1016/j.jtte.2015.05.001.

[16] BSI. (2020). Pd 6694-1:2011+A1:2020 Recommendations for the Design of Structures Subject to Traffic Loading to Bs En 1997-1:2004+A1:2013. In Earth pressures behind integral abutments and end screen walls (pp. 25-30): BSI.

[17] Burke Jr MP. Integral and Semi-Integral Bridges. John Wiley & Sons; 2009.

[18] Burugupelly, N. K. & Dasaka, S. M. (2022, 2022//). Effect of Eps Geofoam on Lateral Earth Pressure Reduction—a Numerical Study Dynamics of Soil and Modelling of Geotechnical Problems, Singapore. 10.1007/978-981-16-5605-7_21.

[19] Caristo, A., Barnes, J., & Mitoulis, S. A. (2018). Numerical Modelling of Integral Abutment Bridges under Seasonal Thermal Cycles. Proceedings of the Institution of Civil Engineers - Bridge Engineering, 171(3), 179-190. 10.1680/jbren.17.00025.

[20] Chen B-C, Fu-yun H, Jun-qing X, Xiao-ye L, Yi-zhou Z, Yong-jian L, et al. Review on research of jointless bridges. J Traffic Transport Eng 2022;2022(5):1–40. https://doi.org/10.19818/j.cnki.1671-1637.2022.05.001.

[21] Chen, Q. (2008). Effects of Thermal Loads on Texas Steel Bridges [PhD Thesis, The University of Texas at Austin]. Texas, USA. http://hdl.handle.net/2152/17802.

[22] O'Loughlin, C., Gaudin, C., & Cassidy, M. (2019). Characterisation of Uwa Superfine Silica Sand. O. G. School. http://hdl.handle.net/11343/251841.

[23] Civjan SA, Kalayci E, Quinn BH, Breña SF, Allen CA. Observed integral abutment bridge substructure response. Eng Struct 2013;56:1177–91. https://doi.org/10.1016/j.engstruct.2013.06.029.

[24] Clayton CRI, Xu M, Bloodworth A. A laboratory study of the development of earth pressure behind integral bridge abutments. Géotechnique 2006;56(8):561–71. https://doi.org/10.1680/geot.2006.56.8.561.

[25] Cosgrove EF, Lehane BM. Cyclic loading of loose backfill placed adjacent to integral bridge abutments. International Journal of Physical Modelling in Geotechnics 2003;3(3):09–16. https://doi.org/10.1680/ijpmg.2003.030302.

[26] Coulomb CA. Essai Sur Une Application Des Regles De Maximis Et Minimis a Quelques Problemes De Statique Relatifs a 1'architecture. Mem Div Sav Acad 1776.

[27] Darley, P., Carder, D. R., & Barker, K. J. (1998). Seasonal Thermal Effects over Three Years on the Shallow Abutment of an Integral Bridge in Glasgow (TRL report 344, Issue. https://books.google.com.au/books?id=nLtjwgEACAAJ.

[28] Dhar S, Dasgupta K. Seismic soil structure interaction for integral abutment bridges: a review. Transportation Infrastructure Geotechnology 2019;6(4):249–67. https://doi.org/10.1007/s40515-019-00081-y.

[29] Dreier D, Burdet O, Muttoni A. Transition slabs of integral abutment bridges. Struct Eng Int 2011;21(2):144–50. https://doi.org/10.2749/101686611X12994961034174.

[30] Duda A, Siwowski T. Pressure evaluation of bridge abutment backfill made of waste tyre bales and shreds: experimental and numerical study. Transp Geotech 2020;24:100366. https://doi.org/10.1016/j.trgeo.2020.100366.

[31] Elgaaly M, Sandford T, Colby C. Testing an integral steel frame bridge. Transportation Research Record(1371) 1992:75–82. https://trid.trb.org/view/371586.

[32] England GL, Tsang NCM, Bush DI. Integral bridges: a fundamental approach to the time-temperature loading problem. Thomas Telford 2000. https://doi.org/10.1680/ibafattttlp.35416.0001.

[33] Farhangi V, Zadehmohamad M, Monshizadegan A, Izadifar M, Moradi MJ, Dabiri H. Effects of geogrid reinforcement on the backfill of integral bridge abutments. Buildings 2023;13(4). https://doi.org/10.3390/buildings13040853.

[34] Fiorentino G, Cengiz C, De Luca F, Mylonakis G, Karamitros D, Dietz M, et al. Integral abutment bridges: investigation of seismic soil-structure interaction effects by shaking table testing. Earthq Eng Struct Dyn 2021;50(6):1517–38. https://doi.org/10.1002/eqe.3409.

[35] Frosch, R. J. & Lovell, M. D. (2011). Long-Term Behavior of Integral Abutment Bridges (FHWA/IN/JTRP-2011/16). 10.5703/1288284314640.

[36] Fu R-H, Briseghella B, Xue J-Q, Aloisio A, Lin Y-B, Nuti C. Experimental and Finite Element Analyses of Laterally Loaded Rc Piles with Pre-Hole Filled by Various Filling Materials in Iabs. Eng Struct 2022;272:114991. https://doi.org/10.1016/j.engstruct.2022.114991.

[37] Hassan MSK, Liyanapathirana DS, Fuentes W, Leo CJ, Hu P. Simulation of soil-structure interaction of integral abutment bridges using advanced constitutive relations. IOP Conference Series: Earth and Environmental Science 2024;1332(1):012020. https://doi.org/10.1088/1755-1315/1332/1/012020.
[38] Hassiotis S, Xiong K. Field Measurements of Passive Pressures Behind an Integral Abutment Bridge. In: In 7th Fmgm 2007: Field Measurements in Geomechanics; 2007. p. 1–12. https://doi.org/10.1061/40940(307)9.
[39] Havinga M, Tschuchnigg F, Marte R, Schweiger H. Small Scale Experiments and Numerical Analysis of Integral Bridge Abutments ICSMGE 2017. Korea: Seoul; 2017.
[40] Hawk, H. (2003). Nchrp Report 483 - Bridge Life-Cycle Cost Analysis. https://onlinepubs.trb.org/onlinepubs/nchrp/nchrp_rpt_483a.pdf.
[41] Highways Agency. (2016). Manual of Contract Documents for Highway Works. In Volume 1 - Specification for Highway Works: Series 600 – Earthworks. London, UK: Highways Agency.
[42] Hoppe EJ. Field Study of Integral Backwall with Elastic Inclusion (FHWA/VTRC 05-R28); 2005. https://rosap.ntl.bts.gov/view/dot/19683.
[43] Horvath JS. Integral-Abutment Bridges: Problems and Innovative Solutions Using Eps Geofoam and Other Geosynthetics (No. CE/GE-00-2); 2000.
[44] Horvath JS. Integral-abutment bridges: a complex soil-structure interaction challenge. In Geotechnical Engineering for Transportation Projects; 2004. p. 460-9. 10.1061/40744(154)31.
[45] Huang F, Li L, Javanmardi A, Zhang H, Izadifar M. Modified calculation method of earth pressure and internal force of the abutment-pile in integral abutment jointless bridges. Archives of Civil and Mechanical Engineering 2022;22(4):205. https://doi.org/10.1007/s43452-022-00533-2.
[46] Huang F, Shan Y, Chen G, Lin Y, Tabatabai H, Briseghella B. Experiment on Interaction of Abutment, Steel H-Pile and Soil in Integral Abutment Jointless Bridges (IAJBs) under Low-Cycle Pseudo-Static Displacement Loads. Appl Sci 2020;10(4):1358. https://doi.org/10.3390/app10041358.
[47] Huntley SA, Valsangkar AJ. Field monitoring of earth pressures on integral bridge abutments. Can Geotech J 2013;50(8):841–57. https://doi.org/10.1139/cgj-2012-0440.
[48] Huntley, S. A. & Valsangkar, A. J. (2018). Nine-Year Field-Monitoring Data from an Integral-Abutment Bridge. Innovations in Geotechnical Engineering: Honoring Jean-Louis Briaud IFCEE 2018, Florida.
[49] INDOT. (2016). Design Manual. In Abutment, Bent, Pier, and Bearing. Indiana, USA: Indiana Department of Transportation.
[50] IOWA DOT. (2023). Lrfd Bridge Design Manual. In Integral Iowa, USA: Iowa Department of Trnasportation - Bridges and Structures Bureau.
[51] Jessee S, Rollins K. Passive Pressure on Skewed Bridge Abutments. 18th International Conference on Soil Mechanics and Geotechnical Engineering. 2013.
[52] Kelly AL, Atadero RA, Mahmoud HN. Life cycle cost analysis of deteriorated bridge expansion joints. Pract Period Struct Des Constr 2019;24(1):04018033. https://doi.org/10.1061/(ASCE)SC.1943-5576.0000407.
[53] Khasawneh, Y. A. (2014). Soil Structure Interaction of Integral Abutment Bridges [PhD Thesis, Purdue University]. Indiana, USA. https://docs.lib.purdue.edu/dissertations/AAI3669413/.
[54] Khodair YA. Lateral Earth Pressure Behind an Integral Abutment. Struct Infrastruct Eng 2009;5(2):123–36. https://doi.org/10.1080/15732470600924706.
[55] Khodair YA, Hassiotis S. Numerical and experimental analyses of an integral bridge. International Journal of Advanced Structural Engineering (IJASE) 2013;5. https://doi.org/10.1186/2008-6695-5-14.
[56] Kim S-H, Ahn J-H, Jung C-Y, Jang J-W, Park Y-H. Behaviour of steel-box semi-integral abutment bridge considering temperature-earth pressure change. International Journal of Steel Structures 2014;14(1):117–40. https://doi.org/10.1007/s13296-014-1011-7.
[57] Kim W, Laman JA. Seven-year field monitoring of four integral abutment bridges. J Perform Constr Facil 2012;26(1):54–64. https://doi.org/10.1061/(ASCE)CF.1943-5509.0000250.
[58] Kim W, Laman JA, Zareian F, Min G, Lee D. Influence of construction joint and bridge geometry on integral abutment bridges. Appl Sci 2021;11(11):5031. https://doi.org/10.3390/app11115031.
[59] Kirupakaran K, Hanlon B, Muraleetharan KK, Miller GA. Field-Measured Response of an Integral Abutment Bridge. In: In Geocongress 2012: State of the Art and Practice in Geotechnical Engineering; 2012. p. 2157–66. https://doi.org/10.1061/9780784412121.221.
[60] Laaksonen A. Temperature and displacement variations of monitored integral bridges fib symposium. Istanbul, Turkey 2023. https://doi.org/10.1007/978-3-031-32511-3_137.
[61] LaFave JM, Brambila G, Kode U, Liu G, Fahnestock LA. Field Behavior of Integral Abutment Bridges under Thermal Loading. J Bridg Eng 2021;26(4):04021013. https://doi.org/10.1061/(ASCE)BE.1943-5592.0001677.
[62] LaFave JM, Riddle JK, Jarrett MW, Wright BA, Svatora JS, An H, et al. Numerical Simulations of Steel Integral Abutment Bridges under Thermal Loading. J Bridg Eng 2016;21(10):04016061. https://doi.org/10.1061/(ASCE)BE.1943-5592.0000919.
[63] Lan, C. (2012). On the Performance of Super-Long Integral Abutment Bridges: Parametric Analyses and Design Optimization [PhD Thesis, University of Trento]. Trento, Italy. http://eprints-phd.biblio.unitn.it/735/.
[64] Lan C, Briseghella B, Fenu L, Xue J, Zordan T. The optimal shapes of piles in integral abutment bridges. Journal of Traffic and Transportation Engineering (English Edition) 2017;4(6):576–93. https://doi.org/10.1016/j.jtte.2017.11.001.
[65] Lawver A, French C, Shield CK. Field performance of integral abutment bridge. Transp Res Rec 2000;1740(1):108–17. https://doi.org/10.3141/1740-14.
[66] Lehane BM. Lateral soil stiffness adjacent to deep integral bridge abutments. Géotechnique 2011;61(7):593–603. https://doi.org/10.1680/geot.9.P.135.
[67] Lin J, Briseghella B, Xue J, Tabatabai H, Huang F, Chen B-C. Temperature monitoring and response of deck-extension side-by-side box girder bridges. J Perform Constr Facil 2020;34(2):04019122. https://doi.org/10.1061/(ASCE)CF.1943-5509.0001399.
[68] Liu G, LaFave JM, Fahnestock LA. Short-term structural response of integral abutment bridge approach slabs subjected to live loading and thermal effects. J Bridg Eng 2024;29(4):04024010. https://doi.org/10.1061/JBENF2.BEENG-6152.
[69] Liu H, Han J, Jawad S, Parsons RL. Literature Review of Causes and Mitigation Techniques for Bumps at Ends of Bridges. In: In Geo-Congress 2020: Geotechnical Earthquake Engineering and Special Topics; 2020. p. 862–71. https://doi.org/10.1061/9780784482810.089.
[70] Liu, H., Han, J., Jawad, S., & Parsons, R. L. (2021a). Experimental Study on Settlement of Backfill in Integral Bridge Abutments Induced by Seasonal Temperature Changes IFCEE 2021, Dallas, Texas. https://doi.org/10.1061/9780784483411.002.
[71] Liu H, Han J, Parsons RL. Mitigation of Seasonal Temperature Change-Induced Problems with Integral Bridge Abutments Using Eps Foam and Geogrid. Geotext Geomembr 2021;49(5):1380–92. https://doi.org/10.1016/j.geotexmem.2021.05.010.
[72] Liu H, Han J, Parsons RL. Effects of Seasonal Temperature Change-Induced Abutment Movements on Backfill Surface Settlements Behind Integral Bridge Abutments – Numerical Analysis. Comput Geotech 2022;149:104884. https://doi.org/10.1016/j.compgeo.2022.104884.
[73] Liu H, Han J, Jawad S, Parsons RL. Effects of traffic loading on seasonal temperature change-induced problems for integral bridge approaches and mitigation with geosynthetic reinforcement. Int J Geomech 2022;22(6):04022082. https://doi.org/10.1061/(ASCE)GM.1943-5622.0002393.
[74] Liu H, Han J, Parsons RL. Geosynthetic reinforcement of backfill behind integral abutments to mitigate approach slab distresses. Eng Struct 2022;269:114772. https://doi.org/10.1016/j.engstruct.2022.114772.
[75] Liu H, Han J, Parsons RL. Integral bridge abutments in response to seasonal temperature changes: state of knowledge and recent advances. Frontiers in Built Environment 2022;8:916782. https://doi.org/10.3389/fbuil.2022.916782.
[76] Liu H, Han J, Parsons RL. Numerical analysis of geosynthetics to mitigate seasonal temperature change-induced problems for integral bridge abutment. Acta Geotech 2023;18(2):673–93. https://doi.org/10.1007/s11440-022-01614-5.
[77] Luo S, De Luca F, De Risi R, Le Pen L, Watson G, Milne D, et al. Challenges and perspectives for integral bridges in the UK: plexus small-scale experiments. Proceedings of the Institution of Civil Engineers - Smart Infrastructure and Construction 2022;175(1):27–43. https://doi.org/10.1680/jsmic.21.00020.
[78] Luo S, Huang Z, Asia Y, De Luca F, De Risi R, Harkness J, et al. Physical and numerical investigation of integral bridge abutment stiffness due to seasonal thermal loading. Transp Geotech 2023;42:101064. https://doi.org/10.1016/j.trgeo.2023.101064.
[79] Madabhushi G. Centrifuge Modelling for Civil Engineers (1 ed.); 2015. CRC Press. 10.1201/9781315272863.
[80] Mahjoubi S, Maleki S. Finite element modelling and seismic behaviour of integral abutment bridges considering soil-structure interaction. Eur J Environ Civ Eng 2020;24(6):767–86. https://doi.org/10.1080/19648189.2017.1421483.
[81] Makino, S., Sega, T., & Nishioka, H. (2024, 20/11/23). Experimental Study of Increasing Earth Pressure on Integral Bridges Subjected to Reciprocal Loads Natural Geo-Disasters and Resiliency, Singapore. 10.1007/978-981-99-9223-2_4.
[82] Marchi A, Gallese D, Gorini DN, Franchin P, Callisto L. On the Seismic Performance of Straight Integral Abutment Bridges: From Advanced Numerical Modelling to a Practice-Oriented Analysis Method. Earthq Eng Struct Dyn 2023;52(1):164–82. https://doi.org/10.1002/eqe.3755.
[83] MassDOT. (2020). Lrfd Bridge Manual. In Design and Analysis of Integral Abutment Bridges. Massachusetts, USA: Massachusetts Department of Transportation, Highway Division.
[84] Mitoulis SA, Palaiochorinou A, Georgiadis I, Argyroudis S. Extending the application of integral frame abutment bridges in earthquake-prone areas by using novel isolators of recycled materials. Earthq Eng Struct Dyn 2016;45(14):2283–301. https://doi.org/10.1002/eqe.2760.
[85] Mitoulis SA. Challenges and Opportunities for the Application of Integral Abutment Bridges in Earthquake-Prone Areas: A Review. Soil Dyn Earthq Eng 2020;135:106183. https://doi.org/10.1016/j.soildyn.2020.106183.
[86] Mofarraj, B. & Zornberg, J. G. (2022). Field Monitoring of Soil-Structure Interaction in Semi-Integral Bridges. In Geo-Congress 2022 (pp. 33-42). 10.1061/9780784484067.004.
[87] Mofarraj B, Zornberg JG. Long-Term Field Monitoring of Lateral Loads in Semi-Integral Bridge Foundations Geo-Congress 2023. California, USA 2023. https://doi.org/10.1061/9780784484685.012.
[88] Morley, D. G., Asia, Y. B., Madabhushi, G. S. P., Thusyanthan, I., & Sakufiwa, D. (2024a, 22/11/23). Influence of relative stiffness on integral bridge design climate change adaptation from geotechnical perspectives, Singapore.
[89] Morley, D. G., Madabhushi, G. S. P., Sakufiwa, D., & Thusyanthan, I. (2024b). Investigation into Soil Ratcheting Behind Integral Bridges Using Centrifuge Modelling. Proceedings of the Institution of Civil Engineers - Bridge Engineering, 0(0), 1-17. 10.1680/jbren.23.00046.
[90] Naji M, Firoozi AA, Firoozi AA. A review: study of integral abutment bridge with consideration of soil-structure interaction. Latin American Journal of Solids and Structures 2020;17(2). https://doi.org/10.1590/1679-78255869.

[91] National Academies of Sciences, E., and Medicine. (2013). Design Guide for Bridges for Service Life (S2-R19A-RW-2). (Strategic Highway Research Program (SHRP 2), Issue. T. N. A. Press. https://onlinepubs.trb.org/onlinepubs/shrp2/SHRP2prepubR19AGuide.pdf.

[92] Ng CWW, Springman SM, Norrish ARM. Centrifuge modeling of spread-base integral bridge abutments. J Geotech Geoenviron Eng 1998;124(5):376–88. https://doi.org/10.1061/(ASCE)1090-0241(1998)124:5(376).

[93] Oesterle, R. G. & Volz, J. S. (2005). Effective Temperature and Longitudinal Movement in Integral Abutment Bridges Integral Abutment and Jointless Bridges (IAJB 2005) Baltimore, Maryland. https://trid.trb.org/view.aspx?id=850811.

[94] Ooi PSK, Lin X, Hamada HS. Field behavior of an integral abutment bridge supported on drilled shafts. J Bridg Eng 2010;15(1):4–18. https://doi.org/10.1061/(ASCE)BE.1943-5592.0000036.

[95] PennDOT. (2019). Design Manual - Structures. In Integral Abutments (pp. Ap.G 1 - Ap.G 23). Pennsylvania, USA: Pennsylvania Department of Transportation.

[96] Pétursson, H. & Collin, P. (2006). Innovative Solutions for Integral Abutments. International workshop on the bridges with integral abutments : topics of relevance for the INTAB project, Luleå, Sweden.

[97] Pétursson H, Kerokoski O. Monitoring and Analysis of Abutment-Soil Interaction of Two Integral Bridges. J Bridg Eng 2013;18(1):54–64. https://doi.org/10.1061/(ASCE)BE.1943-5592.0000314.

[98] Placek, M. (2022). Estimated Worldwide Motor Vehicle Production from 2000 to 2021. statista.com. Retrieved 03/06 from https://www.statista.com/statistics/262747/worldwide-automobile-production-since-2000/.

[99] Queensland Department of Transport and Main Roads. (2021). Design Criteria for Bridges and Other Structures. In. Queensland, Australia: State of Queensland - Department of Transport and Main Roads.

[100] Rankine WJM. II. On the Stability of Loose Earth. Philos Trans R Soc Lond 1857; 147:9–27. https://doi.org/10.1098/rstl.1857.0003.

[101] Razmi J, McCabe M. Analytical and Computational Modeling of Integral Abutment Bridges Foundation Movement Due to Seasonal Temperature Variations. Int J Geomech 2020;20(3):04019189. https://doi.org/10.1061/(ASCE)GM.1943-5622.0001622.

[102] Sakhare A, Punetha P, Meena NK, Nimbalkar S, Dodagoudar GR. Dynamic behaviour of integral abutment bridge transition under moving train loads. Transp Geotech 2023;40:100989. https://doi.org/10.1016/j.trgeo.2023.100989.

[103] Sandberg, J., Magnino, L., Nowak, P., Wiechecki, M., & Thusyanthan, I. (2020). The Integral Bridge Design Concept for the Third Runway at Heathrow, Uk. Proceedings of the Institution of Civil Engineers - Bridge Engineering, 173(2), 112-120. 10.1680/jbren.19.00044.

[104] Sandford, T. C. & Elgaaly, M. (1993). Skew Effects on Backfill Pressures at Frame Bridge Abutments (0309055644). Transportation Research Record, Issue. https://trid.trb.org/view/389610.

[105] Sigdel LD, Al-Qarawi AS, Leo CJ, Liyanapathirana DS, Hu P. Geotechnical design practices and soil-structure interaction effects of an integral bridge system: a review. Appl Sci 2021;11(15):7131. https://www.mdpi.com/2076-3417/11/15/7131.

[106] Sigdel LD, Al-Qarawi AS, Leo CJ, Liyanapathirana DS, Hu P, Doan V. Response of approach to integral abutment bridge under cyclic thermal movement. In: 6th GeoChina International Conference, Nanchang, China; 2021. 10.1007/978-3-030-80142-7_1.

[107] Sigdel LD, Lu M, Al-qarawi A, Leo CJ, Liyanapathirana S, Hu P. Application of engineered compressible inclusions to mitigating soil-structure interaction issues in integral bridge abutments. J Rock Mech Geotech Eng 2023;15(8):2132–46. https://doi.org/10.1016/j.jrmge.2022.12.033.

[108] Sigdel LD, Lu M, Leo CJ, Liyanapathirana DS, Hu P, Doan V, et al. An experimental investigation into soil-structure interactions of integral bridge abutments due to cyclic translations. Can Geotech J 2023. https://doi.org/10.1139/cgj-2022-0500.

[109] Silva PHS, Costa YDJ, Walter JR, Kouchaki BM, Zornberg JG, Costa CML. Numerical Evaluation of a Semi-Integral Bridge Abutment under Cyclic Thermal Movements. Transp Geotech 2023;39:100938. https://doi.org/10.1016/j.trgeo.2023.100938.

[110] Skorpen, S. & Kearsley, E. (2023, 05/06/23). Thermal Loads and Moments in Reinforced Concrete Integral Bridges Building for the Future: Durable, Sustainable, Resilient, Cham. 10.1007/978-3-031-32519-9_149.

[111] Skorpen, S. A., Kearsley, E. P., & Clayton, C. R. I. (2019). Structural Health Monitoring of an Integral Bridge International Conference on Smart Infrastructure and Construction 2019 (ICSIC), Cambridge, UK. 10.1680/icsic.64669.743.

[112] Skorpen, S. A., Kearsley, E. P., & Kruger, E. J. (2018). Measured Temperature and Shrinkage Effects on a 90 M Long Integral Bridge in South Africa. Proceedings of the Institution of Civil Engineers - Bridge Engineering, 171(3), 169-178. 10.1680/jbren.17.00019.

[113] Springman, S. M., Norrish, A. R. M., & Ng, C. W. W. (1996). Cycling Loading of Sand Behind Integral Bridge Abutments (TRL REPORT 146). https://trid.trb.org/view/464703.

[114] Stastny A, Knittel L, Meier T, Tschuchnigg F. Experimental determination of hypoplastic parameters and cyclic numerical analysis for railway bridge backfills. Acta Geotech 2024. https://doi.org/10.1007/s11440-024-02312-0.

[115] Tabatabai, H., Magbool, H., Glennon, B. M., & Ramirez, D. A. B. (2023, 05/06/23). Estimation of Pile Top Displacements in Integral Abutment Bridges Building for the Future: Durable, Sustainable, Resilient, Cham. 10.1007/978-3-031-32511-3_138.

[116] Tabatabai, H., Magbool, H., Bahumdain, A., & Fu, C. (2017). Criteria and Practices of Various States for the Design of Jointless and Integral Abutment Bridges. Third International Workshop on Jointless Bridges, Washington. https://dc.uwm.edu/cee_facart/9/.

[117] Tapper, L. & Lehane, B. (2005). Lateral Stress Development on Integral Bridge Abutments. Developments in Mechanics and Structures of Materials, Perth.

[118] Tatsuoka F, Hirakawa D, Nojiri M, Aizawa H, Nishikiori H, Soma R, et al. A new type of integral bridge comprising geosynthetic-reinforced soil walls. Geosynth Int 2009;16(4):301–26. https://doi.org/10.1680/gein.2009.16.4.301.

[119] Tatsuoka F, Tateyama M, Koda M, Kojima K-I, Yonezawa T, Shindo Y, et al. Research and Construction of Geosynthetic-Reinforced Soil Integral Bridges. Transp Geotech 2016;8:4–25. https://doi.org/10.1016/j.trgeo.2016.03.006.

[120] Trandafir AC, Erickson BA. Stiffness degradation and yielding of eps geofoam under cyclic loading. J Mater Civ Eng 2012;24(1):119–24. https://doi.org/10.1061/(ASCE)MT.1943-5533.0000362.

[121] Vasconez R, Kustau A, Najm H. An overview of integral abutments: current practices, field monitoring and deck replacement measures. Bridge Struct 2022; 18:27–43. https://doi.org/10.3233/BRS-220196.

[122] Verma, M. & Mishra, S. S. (2021). Non-Linear Soil–Structure Interaction of Multi-Span Reinforced Concrete Integral Bridge. Proceedings of the Institution of Civil Engineers - Bridge Engineering, 174(4), 265-280. 10.1680/jbren.20.00022.

[123] VicRoads. (2022). Btn 010 Integral and Semi-Integral Bridges. In. Victoria, Australia.

[124] VDOT. (2022). Vdot Manual of the Structure and Bridge Division. In Abutments. Virginia, USA.

[125] Walter, J. R., Morsy, A. M., & Zornberg, J. G. (2018). Experimental and Numerical Investigation of Lateral Earth Pressures Generated from Repeated Loading IFCEE 2018 : Developments in Earth Retention, Support Systems, and Tunneling, Orlando, Florida. 10.1061/9780784481608.016.

[126] Wang W, Li C, Rens KL, Nogueira CL. Failure Analysis of Pot Bearings in a Curved Viaduct. J Perform Constr Facil 2020;34(5):04020079. https://doi.org/10.1061/(ASCE)CF.1943-5509.0001463.

[127] Wendner R, Strauss A. Inclined Approach slab solution for jointless bridges: performance assessment of the soil-structure interaction. J Perform Constr Facil 2015;29(2):04014045. https://doi.org/10.1061/(ASCE)CF.1943-5509.0000522.

[128] Wiechecki M, Thusyanthan I, Nowak P, Sandberg J. Soil-Structure Interaction Behind Integral Bridge Abutments. In: Proceedings of the Institution of Civil Engineers - Geotechnical Engineering; 2023. p. 1–14. https://doi.org/10.1680/jgeen.22.00115.

[129] Wijaya H, Rajeev P, Gad E. Effect of Seismic and Soil Parameter Uncertainties on Seismic Damage of Buried Segmented Pipeline. Transp Geotech 2019;21:100274. https://doi.org/10.1016/j.trgeo.2019.100274.

[130] Wood, D. M. (2003). Geotechnical Modelling (1 ed.). CRC press. 10.1201/9781315273556.

[131] Wood, J., Murashev, A., Palermo, A., Al-Ani, M., Andisheh, K., & Goodall, D. (2015). Criteria and Guidance for the Design of Integral Bridges in New Zealand (Research Report 577). https://www.nzta.govt.nz/resources/research/reports/577/.

[132] Xiao Y, Long L, Evans TM, Zhou H, Liu H, Stuedlein AW. Effect of particle shape on stress-dilatancy responses of medium-dense sands. J Geotech Geoenviron Eng 2019;145(2):04018105. https://doi.org/10.1061/(ASCE)GT.1943-5606.0001994.

[133] Xu, M. (2005). The Behaviour of Soil Behind Full-Height Integral Abutments [PhD Thesis, University of Southampton]. Southampton, UK. https://eprints.soton.ac.uk/465742/.

[134] Xu M, Bloodworth AG, Clayton CRI. Behavior of a stiff clay behind embedded integral abutments. J Geotech Geoenviron Eng 2007;133(6):721–30. https://doi.org/10.1061/(ASCE)1090-0241(2007)133:6(721).

[135] Xu M, Clayton CRI, Bloodworth AG. The earth pressure behind full-height frame integral abutments supporting granular fill. Can Geotech J 2007;44(3):284–98. https://doi.org/10.1139/t06-122.

[136] Xu M, Guo J. Dem study on the development of the earth pressure of granular materials subjected to lateral cyclic loading. Comput Geotech 2021;130:103915. https://doi.org/10.1016/j.compgeo.2020.103915.

[137] Xue, J. (2013). Retrofit of Existing Bridges with Concept of Integral Abutment Bridge: Static and Dynamic Parametric Analysis [PhD Thesis, University of Trento]. Trento, Italy. http://eprints-phd.biblio.unitn.it/941/.

[138] Xue J, Briseghella B, Lin J, Huang F, Chen B-C. Design and field tests of a deck-extension bridge with small box girder. Journal of Traffic and Transportation Engineering (English Edition) 2018;5(6):467–79. https://doi.org/10.1016/j.jtte.2018.10.004.

[139] Zadehmohamad M, Bazaz JB. Cyclic behaviour of geocell-reinforced backfill behind integral bridge abutment. Int J Geotech Eng 2017;13(5):438–50. https://doi.org/10.1080/19386362.2017.1364882.

[140] Zadehmohamad M, Bazaz JB, Riahipour R, Farhangi V. Physical modeling of the long-term behavior of integral abutment bridge backfill reinforced with tire-rubber. Int J Geo-Eng 2021;12(1):36. https://doi.org/10.1186/s40703-021-00163-2.

[141] Zorzi G, Artoni R, Gabrieli F. Experiments and Dem Simulations of Granular Ratcheting EPJ Web of Conferences 2017. https://doi.org/10.1051/epjconf/201714003061.